[AMERICAN JOURNAL OF SCIENCE, VOL. 298, OCTOBER, 1998, P. 673–698]

ISOTOPE SYSTEMATICS OF GRANITES AND GNEISSES OF THE NANGA PARBAT MASSIF, PAKISTAN HIMALAYA

CAREY A. GAZIS*, JOEL D. BLUM, C. PAGE CHAMBERLAIN, and MICHAEL POAGE

Department of Earth Sciences, HB 6105, Dartmouth College, Hanover, NH 03755

ABSTRACT. Isotopic analyses of gneisses and anatectic granites from the Nanga Parbat-Haramosh Massif (Pakistan Himalaya), a zone of pronounced thermal activity and recent high-grade metamorphism in the Indian Plate, reveal information about the conditions of granite genesis and the nature of Sr exchange in high-grade gneisses and granites. $^{87}Sr/^{86}Sr$ ratios for both gneisses and granites are extremely high and heterogeneous (0.7721-1.0642), indicating that both granites and gneisses have an ancient metasedimentary crustal source. Whole rock Rb-Sr data for gneisses scatter around a reference isochron with an age of 1.8 Ga. Although the Nanga Parbat leucogranites have similar $^{87}Sr/^{86}Sr$ ratios to the surrounding gneisses, their Nd isotopic compositions ($\epsilon Nd = -23$ to -25) are higher than those of the gneisses and migmatites ($\epsilon Nd = -26$ to -29), indicating that the granites' source is not the presently exposed level of gneisses. This result is consistent with other studies that suggest these granites formed as a result of vapor-absent melting during the recent, rapid uplift of Nanga Parbat.

Biotite and feldspar mineral separate Rb-Sr data for six gneisses and one granite have near-horizontal or negative slopes (and ages) on a Rb-Sr isotopic evolution diagram. This behavior is best explained by: (1) a recent (<5 Ma) local homogenization of Sr isotopes during the young metamorphism; and (2) after peak metamorphism, Sr isotope exchange occurred between biotite and carbonate minerals after feldspar became closed to Sr exchange. This exchange took place within the last 2 my and was mediated by metamorphic or magmatic fluids which augmented Sr exchange with carbonate/calcsilicate lenses and/or deposited secondary calcite veins in the granites and gneisses. This proposed Sr exchange between silicates and carbonates could have significant implications for the interpretation of the seawater Sr curve because it enables carbonate dissolution to contribute radiogenic Sr to the dissolved load in streams.

INTRODUCTION

The Nanga Parbat-Haramosh Massif (NPHM) of the northwestern Himalaya is a zone of pronounced, young thermal and tectonic activity. Geochronologic studies of the high grade gneisses and anatectic granites in NPHM have consistently yielded ages of 10 Ma and younger. These studies used a variety of techniques and minerals, including fission track on apatite (Zeitler, 1985), $^{40}Ar/^{39}Ar$ on biotite, muscovite, and hornblende (Zeitler, 1985; Winslow and others, 1994; George, Reddy, and Harris, 1995), U-Pb on zircon and monazite (Zeitler and Chamberlain, 1991; Zeitler, Chamberlain, and Smith, 1993; Smith, Chamberlain, and Zeitler, 1992), and Rb-Sr on muscovite and biotite (George, Harris, and Butler, 1993; George, Reddy, and Harris 1995; George and Bartlett, 1996). These ages are anomalous among more typical >45 Ma metamorphic ages along the western Himalaya (Maluski and Matte, 1984; Treloar and others, 1989; Chamberlain, Zeitler, and Erickson, 1991). The young ages coincide with a period of rapid denudation at Nanga Parbat, which is believed to have occurred at rates of 3 to 5 mm/yr over the past 3 my (Zeitler, 1985; Madin, Lawrence, and Ur-Rehman, 1989; Zeitler, Chamberlain, and Smith, 1993; Whittington, 1996).

The coincidence of young granites with a period of rapid uplift in the NPHM suggests a cause-effect relationship. Thus, a number of studies were conducted to determine the processes that resulted in granite formation. Several models have been proposed based upon geochemical data, field relationships, and heat flow models (Zeitler and Chamberlain, 1991; George, Harris, and Butler, 1993; Chamberlain and others,

* Current address: Geology Department, Central Washington University, Ellensburg, Washington 98926

1995; Butler, Harris, and Whittington, 1997; Whittington, ms). It has been suggested that some of the granites formed as a result of vapor-absent melting during decompression and rapid exhumation of the NPHM (Zeitler and Chamberlain, 1991; Butler, Harris, and Whittington, 1997; Whittington, ms), whereas other granites may have formed as a result of vapor-present melting (Whittington, ms) possibly due to the infiltration of externally-derived fluids (Chamberlain and others, 1995).

Determining the processes that formed these granites is difficult because of the complicated geologic history of the NPHM. The NPHM rocks may have experienced several periods of metamorphism (Treloar, Wheeler, and Potts, 1994) and deformation (Wheeler, Treloar, and Potts, 1995) before the recent (<10 Ma) uplift and metamorphism. In addition, many of the rocks within the massif may have been overprinted by a recent period of fluid flow (Craw and others, 1994; Chamberlain and others, 1995; Butler, Harris, and Whittington, 1997) which further complicates any interpretation of granite genesis.

We undertook this study to obtain more information about the petrogenesis of the young leucogranites and the effects of any hydrothermal activity on these granites. Our approach was to examine a variety of isotopic systems in individual samples. In this paper, we report Rb-Sr, Sm-Nd, and oxygen isotope data for granites, migmatites, gneisses, carbonates, and calcsilicates within the core of the NPHM. In addition, we present Rb-Sr data for mineral separates from seven of these rocks and for waters from active hot springs within the massif. As such, this work expands on the other isotopic tracer studies of the gneisses and granites in the NPHM (Chamberlain and others, 1995; George, Reddy, and Harris, 1995; George and Bartlett, 1996; Butler, Harris, and Whittington, 1997; Whittington, ms).

In this paper, we show that: (1) the leucogranite dikes and stocks were not derived from the surrounding gneisses, confirming earlier observations that the source of the granites is not at the present erosional level (Butler, Harris, and Whittington, 1997; Whittington, ms); and (2) that the Sr isotope ratios of biotite in both granites and gneisses have been affected by post-metamorphic, fluid-mediated exchange with carbonates. This second conclusion has implications beyond the questions of petrogenesis and metamorphism described above. It is relevant to an ongoing discussion of the sources of riverine Sr in the Himalayas and their contribution to the $^{87}Sr/^{86}Sr$ ratio of seawater.

The Sr isotopic composition of seawater, recorded in marine carbonates, is generally regarded as a proxy for the interplay between chemical weathering on continents and seafloor spreading. A sharp rise in the $^{87}Sr/^{86}Sr$ ratio of seawater over the past 40 my is commonly attributed to the uplift and chemical weathering of the Himalayas (Edmond, 1992). Several studies have established that Sr isotopic compositions of Himalayan rivers, particularly those in the Ganges-Brahmaputra system, carry extremely radiogenic Sr (Palmer and Edmond, 1989; Krishnaswami and others, 1992; Harris and others, 1998). Inasmuch as silicate weathering consumes atmospheric CO_2 whereas carbonate weathering does not, there has been much debate over the lithologic source of that radiogenic Sr and the effect of Himalayan weathering on global climate (Raymo, Ruddiman, and Froelich, 1988; Raymo and Ruddiman, 1992; Krishnaswami and others, 1992; Edmond, 1992; Palmer and Edmond, 1992; Blum and others, 1998; Harris and others, 1998; Singh and others, 1998). Fluid-mediated exchange of Sr between biotite and carbonate is a mechanism by which radiogenic Sr can enter the rivers without substantial silicate weathering and CO_2 consumption. If this biotite-carbonate exchange proves to be a widespread phenomenon, this could greatly change estimates of the influence of Himalayan uplift and weathering on atmospheric CO_2.

GEOLOGIC FRAMEWORK

The Nanga Parbat-Haramosh Massif, located in northeastern Pakistan in the northernmost part of the Western Himalayan Syntaxis, is a north-trending half-window of Indian crust. It is surrounded to the north, east, and west by rocks of the Kohistan-Ladakh island arc (fig. 1), which is made up of late Cretaceous and Eocene plutons, volcanics, amphibolites, and pyroxene granulites (Tahirkheli and others, 1979; Coward and others, 1982, 1986, 1987, 1988; Treloar and Izatt, 1993). The Indian plate rocks of the NPHM were thrust below the Kohistan arc rocks along a major suture, the Main Mantle Thrust (MMT), during the Eocene (Treloar and others, 1989; Butler, Harris, and Whittington, 1992). Locally, the MMT is cut by younger faults such as the Raikot/Liachar fault (Butler and Prior, 1988), exposed along the Indus River on the west side of the NPHM (fig. 1).

The NPHM is made up of high grade gneisses and migmatites, coexisting with anatectic granites. The metamorphic rocks are generally quartzofeldspathic biotite and augen gneisses, but carbonates (marbles and dolomites), calcsilicates, and amphibolites are present in lenses, making up a small percentage (<1 percent) of the outcrop exposure. A few massive carbonate lenses are present, such as the dolomite from which sample CG-95-13 was collected. The metamorphic grade in the massif ranges from upper amphibolite-grade on the northwest margin of the massif to granulite-grade near the summit of Nanga Parbat and in the Stak Valley to the northeast (Misch, 1949; Chamberlain, Jan, and Zeitler, 1989; Pognante, Benna, and Le Fort, 1993; George, ms; Khattak, ms; Winslow, Chamberlain, and Zeitler, 1995). In the Tato drainage (fig. 1), metamorphic assemblages of sillimanite–K-feldspar–quartz–biotite and cordierite–K-feldspar–sillimanite–biotite–quartz are present toward the core of the massif (near Nanga Parbat). Pressure-temperature estimates from some of these high-grade rocks vary from 580° to 700°C and 4.4 to 7.5 kb (Chamberlain, Jan, and Zeitler, 1989; Winslow, Chamberlain, and Zeitler, 1995; Whittington, 1996).

There is considerable controversy over the age of the high grade metamorphism of the Nanga Parbat gneisses. Based on petrologic observations and field relationships along the Indus River, Treloar, Wheeler, and Potts (1994) and Wheeler, Treloar, and Potts (1995) conclude that fabrics and some of the metamorphism of the migmatitic gneisses of the NPHM are pre-Himalayan and possibly even Precambrian. Their argument is based, in part, on the observation that the gneisses and migmatites are cut by basic intrusive sheets which are in turn cut by granitic sheets. Wheeler, Treloar, and Potts (1995) suggest that the basic sheets were formed either in the Permian, correlating with the basic magmatism of the Panjal traps, or in the Proterozoic. In contrast, Smith, Chamberlain, and Zeitler (1992) and Zeitler, Chamberlain, and Smith (1993) suggest that metamorphism is less than 10 Ma, based upon U-Pb ages of monazite and zircon in gneisses. They argue that high-grade metamorphism and anatexis occurred recently during a period of rapid denudation. In light of the Precambrian protolith age and the complex tectonic activity of the region, it is likely that these rocks have undergone multiple episodes of metamorphism and deformation. Thus, the different interpretations of metamorphic ages may be due to the different sampling locations and the different methods used to assess the age of metamorphism.

Throughout the massif there are abundant granitic dikes, migmatites, and stocks. Field observations distinguish at least three generations of granitic rocks in the NPHM. Within the gneiss sequence, there are frequent migmatitic zones, the leucosomes presumably being the first generation of granitic rock. Migmatites are clearly syntectonic with the metamorphic event responsible for the regional gneissic foliation, inasmuch as their fabric is concordant with the gneissic foliation. A second generation of granitic rocks are the tourmaline-bearing leucogranites which occur as small stocks and dikes

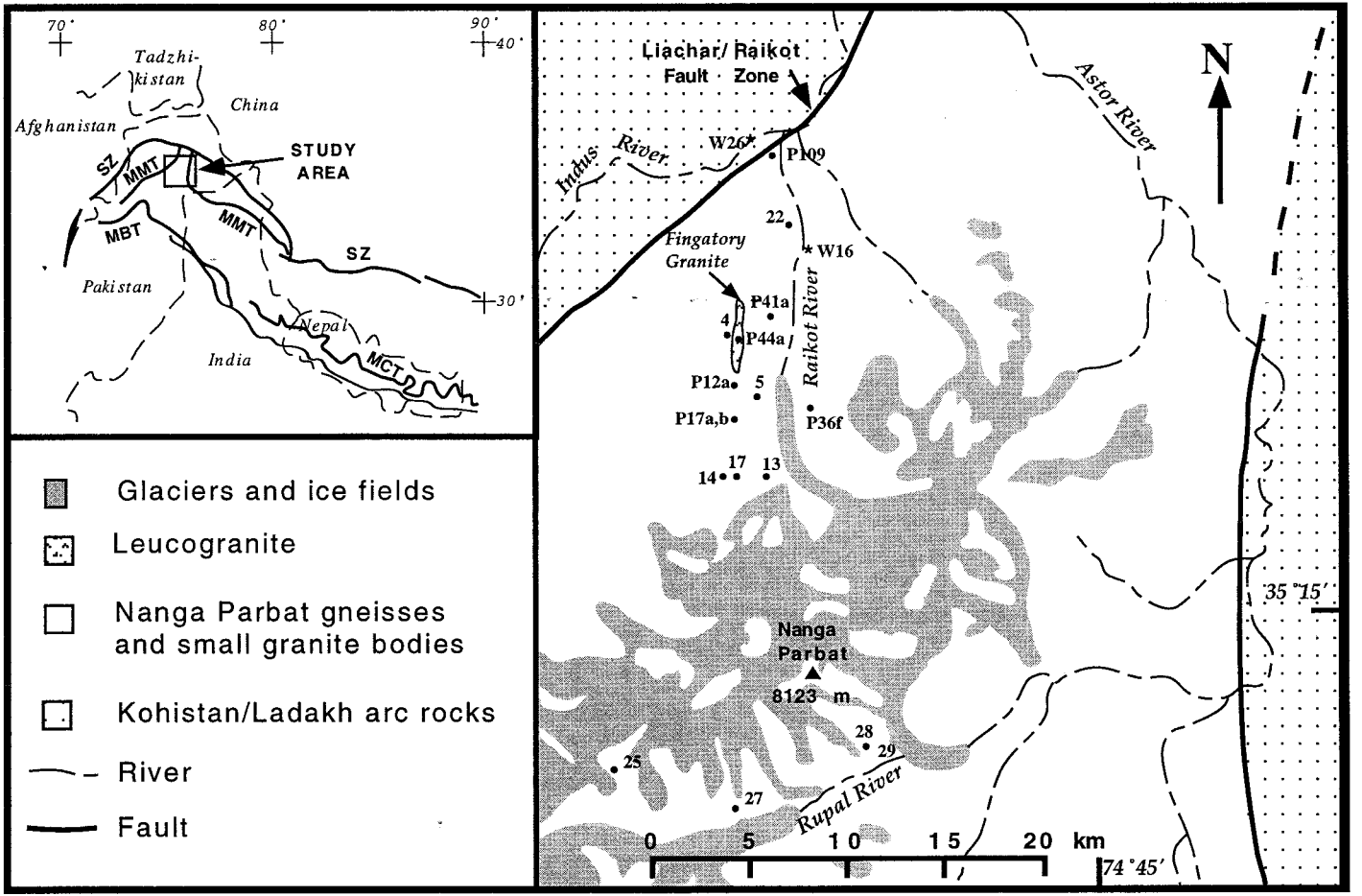

Fig. 1. Location map and geologic sketch map of study area showing sample locations. Fault zones on location map: SZ = Indo-Asian Suture Zone; MMT = Main Mantle Thrust; MBT = Main Boundary Thrust; MCT = Main Central Thrust. On geologic map, black circle = rock sample location; star = hot spring sample location. Sample number abbreviations: ## = CG-95-##; P## = PK-##-90; W## = 95-P-W-##.

throughout the massif. These peraluminous granites, consisting of quartz (20-35 percent), plagioclase (10-20 percent), K-feldspar (30-45 percent), muscovite + biotite (2-10 percent), and tourmaline (<10 percent), are generally discordant with the gneissic foliation. They have been grouped with the High Himalayan leucogranites by Le Fort and others (1987). All the granite samples we analyzed in this study belong to this second generation of leucogranites. The largest stocks are the Jutial Granite, located north of the Indus Gorge (George, Harris, and Butler, 1993) and the Fingatory (or Tato) Granite (Misch, 1949), located on the west side of the Tato drainage, north of Nanga Parbat mountain (fig. 1). Both these bodies are several kilometers in their longest dimension. The third generation of granitic rock are small (<5 cm thick) veins containing quartz, alkali feldspar, and cordierite (frequently altered to chlorite), which overprint the gneissic foliation, particularly along biotite-rich layers (Butler, Harris, and Whittington, 1997; Whittington, ms). These veins occur in outcrop in the Tato drainage near the core of the massif. Boulders containing these veins are commonly seen in moraines of the Raikot glacier and less commonly in the Rupal Valley.

Fluid flow has been an important component of the recent metamorphism and granite genesis at NPHM (Craw and others, 1994; Chamberlain and others, 1995; Butler, Harris, and Whittington, 1997). In a detailed study of rocks from the Tato traverse of the NPHM, Chamberlain and others (1995) found stable isotopic evidence for a dual hydrothermal system consisting of: (1) deep-seated migration of magmatic and metamorphic fluids in the high-grade core of the massif; and (2) relatively near-surface infiltration of meteoric waters along brittle faults. The stable isotopic data (Chamberlain and others, 1995), in part, confirm early work on fluid inclusions by Craw and others (1994), in which inclusions in quartz from late-stage veins were examined to determine the nature of fluid flow during the most recent stages of uplift at Nanga Parbat. Craw and others (1994) concluded that topographically-driven meteoric water has convected through fracture permeability in the brittle part of the crust and has risen to the surface near its boiling point. The presence of active hot springs on the flanks of Nanga Parbat mountain that are isotopically similar (Chamberlain and others, 1995) to local meteoric water (largely stored in glaciers) supports this fluid flow model.

ANALYTICAL TECHNIQUES

We collected rock and hot spring water samples mainly along the Tato and Rupal drainages on the north and south side, respectively, of Nanga Parbat (fig. 1). Our study concentrates on the leucogranite dikes and stocks (Fingatory Granite) described above because volumetrically they are the most important granitic rocks in the massif. In addition, we sampled representative gneiss, migmatite, marble, and calcsilicate rocks from these drainages. We also sampled water from the two main hot spring localities in the study area. The Tato hot springs are located beside Tato village (fig. 1, W16), 22 km north of the summit of Nanga Parbat at an elevation of 2350 m. The Tata Pani hot springs are located on the south side of the Indus River, adjacent to the Raikot fault (fig. 1, W26) at an elevation of 1350 m.

Whole rock samples were powdered in a shatterbox. Biotite, feldspar, and garnet were separated from the 105 to 335 μm size fraction using standard density and magnetic separation techniques. The final mineral separates were hand-picked to ensure high purity. Hot spring samples were filtered through 0.45 μm filters and collected in acid-washed polyethylene bottles.

Twenty to 200 mg of whole rock powders or mineral separates were digested using HF and $HClO_4$ in capped beakers on hotplates until no residue was observed. A small aliquot of each sample was isotopically spiked and concentrations of Sr, Rb, Nd, and Sm were determined by isotope dilution to a precision of about ±10 percent. For a subset of samples, these concentrations were also determined by spiking the entire dissolved

TABLE 1

Sm-Nd data for whole rock samples

sample	Nd (ppm)	Sm (ppm)	Sm/Nd (g/g)	$^{147}Sm/^{144}Nd$	$^{143}Nd/^{144}Nd$	± 2 σ (std. err.)	$^{143}Nd/^{144}Nd_i$ initial*	εNd(0)	εNd(T*)	model age Ga**
Granites										
PK-44a-90†	11.3	2.8	0.25†	0.150	0.511432	± 0.000024	0.511431	–23.5	–23.5	2.14
PK-36f-90†	7.2	1.8	0.25†	0.151	0.511467	± 0.000014	0.511466	–22.8	–22.9	2.10
CG-95-25	5.1	1.4	–	0.166	0.511378	± 0.000012	0.511377	–24.6	–24.6	2.21
CG-95-28	7.3	2.2	–	0.182	0.511451	± 0.000016	0.511450	–23.2	–23.2	2.12
Migmatites										
PK-17b-90-l†	16.0	3.0	0.19†	0.113	0.511164	± 0.000009	0.511157	–28.8	–28.7	2.48
PK-17b-90-m†	23.7	4.3	0.18†	0.110	0.511166	± 0.000014	0.511159	–28.7	–28.6	2.48
Gneisses										
PK-12a-90	50.3	18.0	–	0.216	0.511333	± 0.000014	0.511319	–25.5	–25.5	2.27
PK-109-90	48.8	11.3	–	0.140	0.511277	± 0.000008	0.511268	–26.6	–26.5	2.34
CG-95-5	38.6	10.9	–	0.171	0.511181	± 0.000012	0.511170	–28.4	–28.4	2.46
CG-95-27	49.1	9.0	–	0.111	0.511294	± 0.000030	0.511287	–26.2	–26.1	2.32
CG-95-29	34.7	10.3	–	0.179	0.511251	± 0.000012	0.511239	–27.1	–27.0	2.37

* Initial values calculated assuming ages of 10 Ma. If initial values for granites are calculated assuming an age of 1 Ma, they do not differ significantly from those calculated assuming an age of 10 Ma.

** Model age relative to a depleted mantle reservoir (DM) with $^{143}Nd/^{144}Nd = 0.513114$ and $^{147}Sm/^{144}Nd = 0.222$, assuming average crustal Sm/Nd ratio of 0.17.

† Sm and Nd concentration for these samples were determined to a precision of ±1 percent by isotope dilution and analysis after elution (see text). Sm/Nd ratios for all other samples are not listed because of high uncertainies (±20 percent).

sample and analyzing the appropriate separated fractions after cation exchange elution. The uncertainty on these concentrations is <1 percent. Rb and Sr concentrations for water samples were measured using a high-resolution inductively coupled plasma mass spectrometer (ICP-MS) with an estimated precision of ≤5 percent.

Rubidium, Sr, Sm, and Nd were separated from the whole rock digests using quartz cation exchange columns. Dowex AG50 X8 resin (200-400 mesh) was first used to separate Rb, Sr, and rare earth element (REE) fractions, and then a second column with AG50 X8 resin (<400 mesh) was used to separate Sm and Nd fractions. Because of the high Rb/Sr ratios of these rocks, strontium fractions were routinely re-eluted through small columns loaded with strontium specific resin (EIChroM Sr · Spec). To obtain Sr from hot spring water samples, a portion of each sample was evaporated and eluted twice using the Sr specific resin. Sr isotopic compositions were determined using a VG Sector single collector thermal ionization mass spectrometer (TIMS). A Finnigan MAT 262 TIMS with 8 collectors was used to determine Nd isotope ratios. Sr and Nd isotope ratios were normalized to $^{86}Sr/^{88}Sr = 0.1194$ and $^{146}Nd/^{144}Nd = 0.7219$, respectively. Thirty-seven analyses of the NBS 987 Sr standard and 26 analyses of the Caltech nNdβ standard during the time of this study gave isotopic ratios of $^{87}Sr/^{86}Sr = 0.710202 \pm 0.000021$ and $^{143}Nd/^{144}Nd = 0.511893 \pm 0.000008$ (2σ). Total procedural blanks were <100 ng for Sr and <20 ng for Nd.

An aliquot of each whole rock digestion and of the hot spring samples was analyzed for major element concentrations using an inductively coupled plasma optical emission spectrometer (ICP-OES). The estimated precision of this method is ≤5 percent based on measurement of calibration standards.

Oxygen isotope compositions of these whole rocks were determined using a conventional BrF_5 extraction line at Dartmouth College. Powdered samples were kept in a drying oven overnight at approx 80°C and loaded into nickel rod reaction bombs in a drybox. Bombs were evacuated under high vacuum for 2 hrs at 300°C to minimize contamination by atmospheric moisture. Samples were then reacted with excess BrF_5 for ~10 hrs at 560°C. Liberated oxygen was converted to CO_2 in the presence of heated graphite, and the resultant CO_2 was cryogenically purified and analyzed on a Finnigan MAT 252 gas source magnetic sector mass spectrometer. $^{18}O/^{16}O$ ratios are converted to the standard δ-notation as permil (‰) difference from Standard Mean Ocean Water (SMOW). Analytical precision is ~0.25 permil (1σ), based on 12 analyses of an internal laboratory quartz standard.

RESULTS

Major element compositions for 13 whole rock and 2 hot spring samples are listed in table 2. Granites have bulk compositions within the range typical of peraluminous granites (Hess, 1989, p. 228). Gneisses and migmatites have a wide range of bulk compositions, corresponding to a wide range of modal mineralogies, from 50 wt percent SiO_2 in a garnet gneiss to 77 wt percent SiO_2 in the leucosome of a migmatite. Hot spring waters are rich in Na, Si, and F and contain relatively low concentrations of Fe and Mg. The presence of high concentrations of Na, Si, and F is consistent with water-rock interaction with the high-grade gneisses that contain abundant plagioclase as well as biotites with unusually high F contents (Winslow, Chamberlain, and Zeitler, 1995).

Oxygen and Sr isotopic compositions and Rb and Sr concentrations of 21 whole rock samples are given in table 3. With the exception of one sample, which appears to be isotopically altered by hydrothermal fluids (CG-95-27), gneisses and migmatites have whole rock $\delta^{18}O$ values between +9.0 and +13.6 permil, while granites $\delta^{18}O$ values range from +8.6 to +10.3 permil. Chamberlain and others (1995) also observed that Nanga Parbat granites appear to have lower $\delta^{18}O$ values than the surrounding gneisses. $^{87}Sr/^{86}Sr$ ratios of Nanga Parbat gneisses, migmatites, and granites are high and ex-

TABLE 2

Major element compositions of whole rock and hot spring samples

Sample	Al_2O_3 (wt%)	CaO (wt%)	Fe_2O_3 (wt%)	K_2O (wt%)	MgO (wt%)	MnO (wt%)	Na_2O (wt%)	TiO_2 (wt%)	SiO_2 (wt%)
granites									
CG-95-25	14.56	0.83	0.73	4.22	0.08	0.02	3.23	0.04	75.3*
CG-95-28	14.61	1.03	0.79	2.70	0.07	0.02	3.91	0.05	75.8*
PK-44a-90	13.20	1.32	1.02	5.35	0.08	0.03	3.52	0.08	74.4*
migmatites									
PK-17b-90-m**	11.87	1.06	2.4	4.16	0.92	0.03	2.42	0.44	73.3
gneisses									
CG-95-27	15.29	1.69	5.35	4.74	1.32	0.05	2.35	0.71	67.5*
PK-12a-90	14.45	2.24	6.52	3.79	1.20	0.09	2.27	0.84	67.6*
CG-95-4	14.76	2.32	7.06	4.43	1.71	0.06	2.10	0.89	65.7*
CG-95-14	24.20	0.75	12.80	3.58	3.55	0.24	0.65	0.75	52.5*
CG-95-17	14.51	3.15	18.69	2.69	4.75	0.27	0.87	3.43	50.6*
CG-95-5	21.62	0.29	10.73	3.99	3.04	0.21	0.50	0.68	57.9*
PK-41a-90	14.92	2.97	4.23	2.23	1.05	0.04	3.07	0.40	70.1*
PK-41a-90**	14.05	2.91	4.01	2.37	0.98	0.03	3.27	0.40	65.7
CG-95-29	14.08	1.28	4.16	4.37	1.14	0.03	2.64	0.52	70.8*

Sample	pH	Al (ppm)	Ca (ppm)	Fe (ppm)	K (ppm)	Mg (ppm)	Mn (ppm)	Na (ppm)	Si (ppm)	F (ppm)	Cl (ppm)	SO_4 (ppm)
hot springs												
95-P-W-16	8.9	0.028	1.42	b.d.†	17.2	0.031	b.d.†	283.0	102.1	25.1	98.1	54.6
95-P-W-26	8.7	0.057	3.17	b.d.†	3.4	0.030	b.d.†	201.3	31.3	26.1	38.4	175.5

* SiO_2 concentration calculated by difference assuming 1% LOI

**Analysis of lithium metaborate digestion performed by ICP-OES.

† b.d.–below detection limit.

TABLE 3

Rb-Sr and oxygen isotope data for whole rocks and hot springs

Sample	description, location	Rb (ppm)	Sr (ppm)	Rb/Sr (g/g)	$^{87}Rb/^{86}Sr$	$^{87}Sr/^{86}Sr$	± 2 σ (std err.)	$^{87}Sr/^{86}Sr_i$ initial**	$\delta^{18}O$ (‰)
Granites									
PK-44a-90	Fingatory granite, near Fairy Meadows (Tato drainage)	424.8	63.0	6.7	19.85	0.88776	± 0.00005	0.88748	8.6
PK-36f-90	granite dike (Tato drainage)	362.0	45.1	8.0	23.64	0.89091	± 0.00005	0.89057	9.4
CG-95-25	leucogranite, S. of Mazino pass (Rupal drainage)	255.0	28.3	9.0	26.42	0.84327	± 0.00003	0.84289	9.1
CG-95-28	coarse-grained tourmaline granite, Tap meadow (Rupal)	254.1	24.4	10.4	30.98	0.99671	± 0.00005	0.99627	10.3
Migmatites									
PK-17b-90-l	migmatite - leucosome (Tato drainage)	98.3	65.5	1.5	4.41	0.86752	± 0.00005	0.86689	9.8
PK-17b-90-m	migmatite - melanosome (Tato drainage)	226.8	94.5	2.4	7.05	0.86597	± 0.00003	0.86587	10.6
CG-95-22	garnet-bearing migmatite - leucosome, 2 km S. of Tato village	131.6	184.4	0.7	2.09	0.85280	± 0.00002	0.85277	10.7
Gneisses									
PK-12a-90	biotite gneiss (Tato drainage)	184.8	157.0	1.2	3.44	0.82358	± 0.00004	0.82353	9.7
PK-17a-90	biotite gneiss, contains sillimanite - Tato shear zone	221.9	110.6	2.0	5.87	0.82516	± 0.00003	0.82508	9.0
PK-41a-90	altered biotite gneiss - Tato shear zone	98.4	257.2	0.4	1.11	0.77209	± 0.00003	0.77207	10.1
PK-109-90	augen gneiss, ≈2 km from Raikhot fault (Tato drainage)	378.9	78.4	4.8	14.47	1.06418	± 0.00004	1.06397	10.4
CG-95-4	biotite gneiss, 200 ft above Fingatori gr. (Tato drainage)	222.5	162.0	1.4	4.02	0.81828	± 0.00004	0.81822	10.1
CG-95-5	garnet-bearing biotite gneiss (Tato drainage)	182.4	62.5	2.9	8.59	0.88387	± 0.00003	0.88375	12.8
CG-95-14	garnet gneiss, large garnets, Jilliper ridge (Tato drainage)	184.1	72.5	2.5	7.45	0.85103	± 0.00003	0.85092	13.6
CG-95-17	garnet gneiss, ≈30% garnet, Jilliper ridge (Tato drainage)	170.2	30.2	5.6	16.48	0.81700	± 0.00003	0.81677	10.5
CG-95-27	augen gneiss, near lower Mazino base camp (Rupal)	288.9	117.4	2.5	7.26	0.91255	± 0.00005	0.91245	5.7
CG-95-29	biotite gniess, country rock adjacent to CG-95-28 (Rupal)	248.5	122.1	2.0	5.99	0.88704	± 0.00003	0.88695	10.0
PK/NR 19-89	gneiss - 25km N. of Tato (Indus River valley)	118.3	79.5	1.5	4.33	0.76806	± 0.00002	0.76800	11.7
Carbonates									
CG-95-13	dolomite, ridge east of S. Jilliper peak (Tato drainage)	5.3	15.1	0.35	1.02	0.73326	± 0.00003		14.9
JDB-TC	calcite, from block of float near Tato village	0.7	180.4	0.00	0.01	0.70580	± 0.00004		17.3
JDB-CS	carbonate minerals in calcsilicate, float near Tato village	6.3	268.6	0.02	0.07	0.80300	± 0.00004		19.1
Travertine Deposits									
PK-NP-4-C-92	precipitate from hot spring at Tato village	129.6	114.4	1.1	3.32	0.82435	± 0.00005		
Hot spring waters		(ppb)	(ppb)						
PK-NP-4-E-92	Tato hot spring, same location as 95-P-W-16 (fig. 1)	113.8	17.5	6.50	19.00	0.80979	± 0.00002		
PK-1-E-92	Tata Pani hot spring, same loc. as 95-P-W-26 (fig. 1)	38.6	33	1.17	3.43	0.83547	± 0.00006		
Kohistan		(ppm)	(ppm)						
PK-90-KK-16	gabbro - Kohistan arc	0.09	37.9	0.00	0.01	0.70444	± 0.00003		

** Ages used to determine initial $^{87}Sr/^{86}Sr$: 1 Ma for granite, 10 Ma for gneisses and migmatites.

tremely variable,ranging from 0.7681 to 1.0642. Three carbonate/calcsilicate samples have lower $^{87}Sr/^{86}Sr$ ratios, between 0.7058 to 0.8030. Hot spring waters and travertine deposits have values ranging from 0.8098 to 0.8355. $^{87}Rb/^{86}Sr$ ratios of nearly all NPHM granites and gneisses analyzed are quite high, generally greater than one and as high as 30. All the granites we analyzed have higher $^{87}Rb/^{86}Sr$ ratios than the surrounding gneiss.

Mineral separate Rb-Sr data are listed in table 4. The range of $^{87}Sr/^{86}Sr$ ratios for coexisting minerals within individual rock samples is small relative to the range between separate samples. In five out of seven samples, biotite, the mineral with the highest Rb/Sr ratio, has a lower $^{87}Sr/^{86}Sr$ ratio than the coexisting feldspar or whole rock. All four garnets analyzed have higher Rb/Sr ratios and lower $^{87}Sr/^{86}Sr$ ratios than coexisting feldspar. Whole rock Sm-Nd data for 11 samples (table 1) reveal that these rocks have a narrow range of $^{143}Nd/^{144}Nd$ ratios. Gneisses and migmatites analyzed have distinctly different $^{143}Nd/^{144}Nd$ values (0.51116-0.51132) than the granites ($^{143}Nd/^{144}Nd$ = 0.51138-0.51147).

AGE OF GNEISS PROTOLITH

Determining the geologic history of the NPHM is complicated because several episodes of intense metamorphism and deformation have obscured many geologic relationships. Thus, any constraints on the source and nature of the protolith of the NPHM gneisses are extremely valuable. In general, the protolith for the Nanga Parbat gneisses is varied, coming from two main sources: (1) a stratigraphic sequence of

TABLE 4

Mineral separate Rb-Sr data

sample	description	Rb (ppm)	Sr (ppm)	Rb/Sr (g/g)	$^{87}Rb/^{86}Sr$	$^{87}Sr/^{86}Sr$	± 2 σ (std err.)
PK-12a-90	biotite gneiss	184.8	157.0	1.2	3.44	0.82358	± 0.00004
PK-12a-90-F	biotite gneiss - feldspar	341.5	278.6	1.2	3.59	0.82393	± 0.00005
PK-12a-90-B	biotite gneiss - biotite	736.4	16.7	44.1	128.9	0.81643	± 0.00003
PK-12a-90-GA	biotite gneiss-garnet	5.4	1.9	2.8	8.31	0.81465	± 0.00003
CG-95-17	garnet gneiss, Jilliper ridge	170.2	30.2	5.6	16.48	0.81699	± 0.00003
CG-95-17-F	garnet gneiss - feldspar	2.4	128.2	0.02	0.05	0.81668	± 0.00002
CG-95-17-B	garnet gneiss - biotite	528.2	3.5	150.9	441.4	0.81813	± 0.00005
CG-95-17-GA	garnet gneiss - garnet	1.3	1.3	1.1	3.08	0.81277	± 0.00007
CG-95-14	garnet gneiss, Jilliper ridge	184.1	72.5	2.5	7.45	0.85103	± 0.00003
CG-95-14-F	garnet gneiss - feldspar	107.6	312.2	0.34	1.01	0.85622	± 0.00004
CG-95-14-B	garnet gneiss - biotite	619.1	6.6	93.8	274.2	0.81103	± 0.00006
CG-95-14-GA	garnet gneiss - garnet	5.5	1.9	2.9	8.48	0.83056	± 0.00003
CG-95-22	migmatite, N. of Tato	131.6	184.4	0.7	2.09	0.85280	± 0.00002
CG-95-22-F	migmatite - feldspar	195.0	261.0	0.7	2.19	0.85306	± 0.00003
CG-95-22-B	migmatite - biotite	698.0	4.6	151.7	444.7	0.84002	± 0.00003
CG-95-22-GA	migmatite - garnet	1.8	1.0	1.8	5.28	0.85265	± 0.00002
PK-109-90	augen gneiss	378.9	78.4	4.8	14.47	1.06418	± 0.00004
PK-109-90-F	augen gneiss - feldspar	662.1	151.9	4.4	13.06	1.06952	± 0.00004
PK-109-90-B	augen gneiss - biotite	1335.7	13.4	99.7	297.9	1.04115	± 0.00002
PK-41A-90	altered gneiss - Tato shear zone	98.4	257.2	0.4	1.11	0.77209	± 0.00003
PK-41A-90-F	altered gneiss- feldspar	240.8	416.2	0.6	1.68	0.77205	± 0.00003
PK-41A-90-B	altered gneiss - biotite	638.5	4.3	148.5	432.5	0.77457	± 0.00002
PK-44a-90	Fingatory granite, Fairy Mdws	424.8	63	6.7	19.85	0.88776	± 0.00005
PK-44A-90-F	Fingatory granite - feldspar	925.6	72.8	12.7	37.43	0.88636	± 0.00001
PK-44A-90-B	Fingatory granite - biotite	2388.1	1.4	1706	5020	0.88325	± 0.00006

predominantly pelitic sediments with minor amounts (~1 percent) of calcareous sediments and mafic volcanic rocks, and (2) orthogneisses consisting of highly deformed granitic igneous rocks. Previous research on xenocrystic components of zircons in these gneisses suggests that at least some of this protolith is of Precambrian age. A paragneiss unit (Shengus gneiss) yields zircon U-Pb ages of approx 400 to 500 Ma (Zeitler and others, 1989) and a orthogneiss unit (Iskere gneiss) gives a U-Pb age of approx 1.85 Ga (Zeitler and Chamberlain, 1991; Zeitler, Chamberlain, and Smith, 1993).

Our Rb-Sr data provide additional support for a Precambrian protolith: 13 out of 14 whole rock data scatter around a reference isochron for 1.8 Ga with $^{87}Sr/^{86}Sr_{initial} = 0.710$ (fig. 2). Data for Nanga Parbat gneisses from George, Harris, and Butler (1993) (also shown in fig. 2) also scatter around this reference isochron as do data for samples collected along the Liachar shear zone (George and Bartlett, 1996). Most of the data are bracketed by 1.4 and 2.2 Ga reference isochrons. We do not believe that any of these lines represents a whole rock isochron, which would assume initial Sr isotope homogeneity, but rather that the source rocks for Nanga Parbat gneisses are Precambrian, with ages between 1.4 and 2.2 Ga. The extremely high $^{87}Sr/^{86}Sr$ and low $^{143}Nd/^{144}Nd$ ratios of the Nanga Parbat gneisses are also consistent with a Precambrian protolith.

Alternatively, the protolith for these rocks may be older than 2.2 Ga, as the model Nd ages (table 1, 2.3 to 2.5 Ga for gneisses) might suggest, but has undergone a major thermal event around 1.8 Ga. These model ages represent an estimate of when the melts from which the gneisses were eventually derived were separated from the mantle. These ages were calculated assuming an average crustal Sm/Nd ratio of 0.17 (Taylor and McLennan, 1985), a ratio that has clearly not been maintained until the present for the granites.

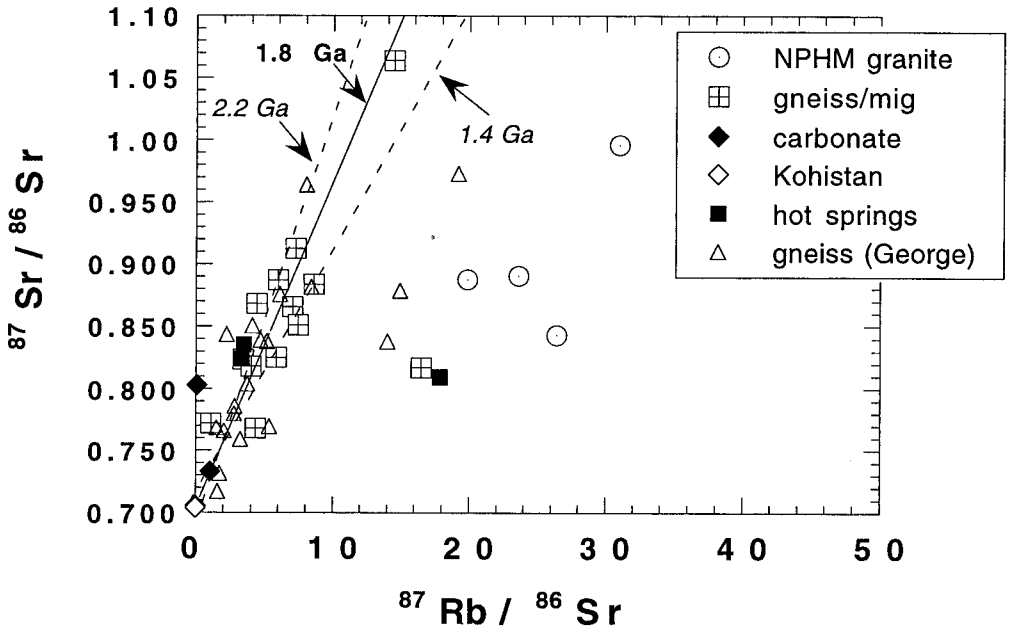

Fig. 2. $^{87}Rb/^{86}Sr$-$^{87}Sr/^{86}Sr$ isochron diagram with data from Nanga Parbat granites (open circles), gneisses and migmatites (crossed squares), carbonates/calcsilicates (black diamonds), Kohistan gabbro (open diamond), hot spring waters and precipitate (black squares). Data from George, Harris, and Butler (1993) for Nanga Parbat gneisses are also shown (open triangles). Solid line is a 1.8 Ga reference isochron, dashed lines are 1.4 and 2.2 Ga reference isochrons. All have $^{87}Sr/^{86}Sr_{initial} = 0.710$.

PETROGENESIS OF NANGA PARBAT LEUCOGRANITES

Recently, a number of isotopic studies have been undertaken to determine the source of granites in the NPHM. These studies suggest that the granitic migmatite seams in the high-grade core of the massif formed in vapor-present conditions (Whittington, ms) possibly during fluid infiltration (Chamberlain and others, 1995). In contrast, the leucogranite dikes and stocks that are found throughout the massif are believed to have formed during vapor-absent conditions (George, Harris, and Butler, 1993; Whittington, ms) as a result of decompression melting during rapid uplift.

Our study concentrated on the leucogranite dikes and stocks located in the high-grade core of the massif, because earlier studies of these granites showed that they had distinctly different oxygen isotope values than the gneisses (Chamberlain and others, 1995), and it was unclear whether this difference was a result of post-magmatic alteration by fluids or derivation of granites from an isotopically distinct source.

Several observations based on our data and data from George, Harris, and Butler (1993), Chamberlain and others (1995), and Whittington (ms) must be explained by any petrogenetic model for the Nanga Parbat leucogranites dikes and stocks:

1. Granites have a significantly higher Rb/Sr ratio than their host gneisses (fig. 2). These Rb/Sr ratios, along with their Ba/Sr ratios, have been attributed to vapor-absent incongruent melting of muscovite (George, Harris, and Butler, 1993; Whittington, ms).

2. The whole rock $^{87}Sr/^{86}Sr$ ratios of the granites (0.8432-0.9967) are quite high and fall within the range of $^{87}Sr/^{86}Sr$ of the gneisses (0.7721-1.0642). In addition, present day Nd isotopic ratios for granites ($\epsilon Nd = -23$ to -25) are close to but slightly higher than those of the gneisses and migmatites ($\epsilon Nd = -26$ to -29). Whittington (ms) observed similar variations in $^{143}Nd/^{144}Nd$ and $^{87}Sr/^{86}Sr$ ratios for leucogranite stocks in the high-grade core of the massif. Data from George, Harris, and Butler (1993) for granites and gneisses from elsewhere in the massif are also in general agreement with our data: Nd isotopic ratios for the Jutial granite ($\epsilon Nd = -24$ to -27) are slightly lower than our granite values; four out of five gneisses have ϵNd between -26 and -32, and one has an anomalously high ϵNd of -20.

3. Excluding samples that have obviously undergone typical hydrothermal oxygen isotope exchange, the granites have an average whole rock $\delta^{18}O$ of 9.1 ± 1.5 permil (1σ, $n = 26$), while the average whole rock $\delta^{18}O$ of the unaltered host gneisses is 11.5 ± 1.0 permil ($1\ \sigma$, $n = 21$; Chamberlain and others, 1995). Although these averages overlap within 2σ, a standard T-test confirms that the differences between the means are statistically significant (significance level $\alpha = 0.01$). Thus, the granites appear to have whole rock $\delta^{18}O$ values approx 2 permil lower than the adjacent gneisses.

The granites in the core of the massif are isotopically distinct from the migmatites. The melanosome and leucosome from a single migmatite sample (PK-17b-90) are nearly identical in their Sr and Nd isotopic composition and distinctly different from that of the granites (fig. 3). Thus, it does not appear that the granites are related to the migmatite leucosomes.

It is unlikely that the lower $\delta^{18}O$ of the granites is a result of subsolidus interaction with meteoric water. The quartz-feldspar and quartz-biotite data for granites presented in Chamberlain and others (1995) vary considerably because of the many small bodies sampled, but for the majority of granites analyzed mineral oxygen isotopes have equilibrated at temperatures between 500° and 900°C. These mineral pairs do not show evidence for interaction with any substantial amounts of meteoric water, in that feldspar $\delta^{18}O$ values have not been lowered as would be expected after interaction with meteoric waters at temperatures $\geq$300°C (Criss, Gregory, and Taylor, 1987). We, therefore, suggest that the relatively low $\delta^{18}O$ values of the granites reflect the isotopic composition of their source, which is deeper than the presently exposed gneisses; this conclusion is consistent with the differing ϵNd values of the granites and gneisses. These low $\delta^{18}O$

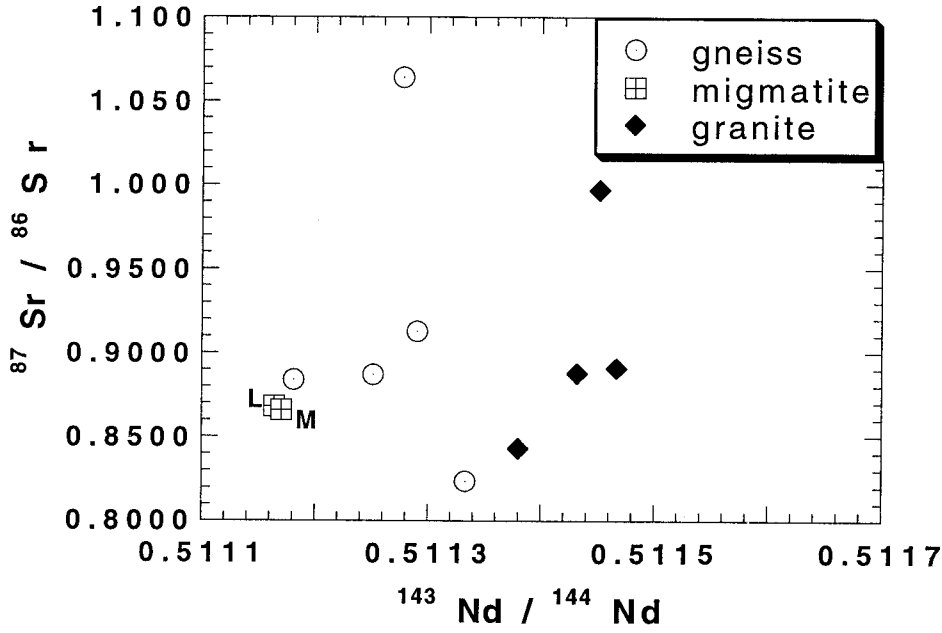

Fig. 3. $^{87}Sr/^{86}Sr$-$^{143}Nd/^{144}Nd$ plot of Nanga Parbat gneisses (open circles), migmatites (crossed squares, L = leucosome; M = melanosome), and granites (black diamonds).

values could either be the result of water-rock interaction in the source area prior to melting or by a greater proportion of orthogneisses in the source rock.

Based on our data, two conclusions can be drawn as to the origin of the Nanga Parbat leucogranite dikes and stocks in the core of the massif. First, the extremely high $^{87}Sr/^{86}Sr$ ratios and low ϵNd of the Nanga Parbat granites confirm that they are crustal in origin and have no observable primitive magmatic component. Second, geochemical evidence suggests that the source rock for the leucogranite dikes and stocks is not the presently exposed level of gneisses, consistent with other studies that suggest the leucogranite stocks formed from rocks not presently exposed on the erosional surface (Butler, Harris, and Whittington, 1997).

It is useful to compare the geochemistry of granites at Nanga Parbat with granites elsewhere in the Himalaya because of the tectonic significance of granite genesis. The leucogranites of NPHM are roughly in line with a belt of geochemically similar anatectic granites known as the High Himalayan leucogranites which run along the core of the mountain range (Le Fort and others, 1987). The petrogenesis of the High Himalayan leucogranites has been discussed by a number of workers (Debon and others, 1986; Le Fort and others, 1987; Scaillet, France-Lanord, and Le Fort, 1990; Inger and Harris, 1993; Harris, Inger, and Massey, 1993; Harris, Ayres, and Massey, 1995), all of whom agree that the granites have a sedimentary crustal source. Le Fort and others (1987) propose a model for the petrogenesis of High Himalayan leucogranites in which they are fluxed by volatiles given off during dehydration of rocks in the footwall of major crustal fault complexes such as the Main Central Thrust (MCT). These fluids are believed to have generated melts in the hanging wall and then emplaced at major disharmonic zones above the fault. Harris, Ayres, and Massey (1995) offer a different petrogenetic model: Based on distributions of Rb, Sr, and Ba between minerals in leucogranites and Himalayan mica schists, they conclude that the High Himalayan granites were formed

by fluid-absent muscovite breakdown in a pelitic source at midcrustal levels. They argue that fluid-present melting would produce higher melt fractions with lower Rb/Sr ratios than those observed.

The leucogranites at Nanga Parbat, which consist of quartz, plagioclase, K-feldspar, muscovite ± biotite, and tourmaline, are mineralogically similar to the High Himalayan leucogranites. This similarity together with their position near the axis of the high Himalayas led Le Fort and others (1987) to group the Nanga Parbat leucogranites together with the High Himalayan leucogranites. However, the geochemical data collected since 1987 suggests that the Nanga Parbat leucogranites do not have as much in common with the High Himalayan leucogranites as was previously assumed, for the following reasons:

First, the granites at Nanga Parbat are much younger than the High Himalayan leucogranites. High Himalaya granites typically yield K-Ar and Rb-Sr ages of 12 to 20 Ma (Ferrara, Lombardo, and Tonarini, 1983; Le Fort and others, 1987; Deniel and others, 1987). In contrast, Ar-Ar and U-Pb ages for the leucogranites at Nanga Parbat are between 1 and 10 Ma (Zeitler and Chamberlain; 1991; Zeitler, Chamberlain, and Smith, 1993; Winslow and others, 1994).

Second, the Nanga Parbat granites have a distinctly different isotopic signature than the other High Himalayan leucogranites (fig. 4). Initial $^{87}Sr/^{86}Sr$ ratios (calculated for 20 Ma) for ten High Himalayan leucogranites all fall within the range of 0.724 to 0.826. Initial $^{87}Sr/^{86}Sr$ ratios for four Nanga Parbat granites are substantially higher, ranging from 0.843 to 0.996 (calculated for 1 Ma; for comparison, the range for 20 Ma is 0.836-0.988). Similarly, oxygen isotope compositions of High Himalayan granites and Nanga Parbat granites are different. Measured $\delta^{18}O$ values for High Himalayan granites

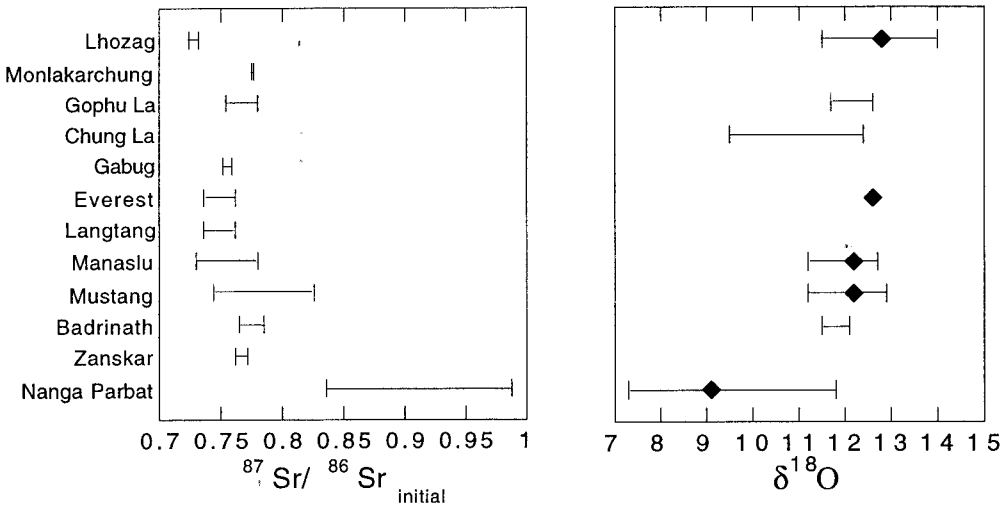

Fig. 4. Comparison of $^{87}Sr/^{86}Sr_{initial}$ ratios (A) and $\delta^{18}O$ values (B) for High Himalayan leucogranites and Nanga Parbat leucogranites. Ranges of measured values are bracketed. Black diamonds represent mean $\delta^{18}O$ values. Granites that have clearly been isotopically altered by hydrothermal fluids are excluded. Nanga Parbat data from this study and Chamberlain and others (1995). Data sources for High Himalayan leucogranites: Lhozag-Debon and others (1986), Sheppard and others (1983), Sheppard (1986); Monlakarchung-Dietrich and Gansser (1981), Gansser (1983); Gophu La-Dietrich and Gansser (1981), Gansser (1983); Ferrara, Lombardo, and Tonarini (1983); Gabug-Wang and others (1981); Everest-Ferrara, Lombardo, and Tonarini (1983), Vidal and others (1984); Langtang-Inger and Harris (1993); Massey, Harmon, and Harris (1994); Manaslu-Deniel and others (1987), Vidal and others (1984), France-Lanord, Sheppard, and Le Fort (1988); Mustang-Vidal and others (1984); Badrinath-Scaillet, France-Lanord, and Le Fort (1990), Blattner, Dietrich, and Gansser (1983); Zanskar-Searle and Fryer (1986).

range from +11.0 to +14.0 permil. Nanga Parbat granites, which do not display clear evidence for subsolidus oxygen isotope exchange, have $\delta^{18}O$ values between +7.3 and +12.3 permil, more variable and generally lower than their High Himalayan counterparts (fig. 4). In addition to these isotopic differences, studies of the trace element chemistry show that Nanga Parbat leucogranites have higher Rb/Sr ratios and are enriched in U and Th, which may reflect high heat production in the granites' source rocks (George, Harris, and Butler, 1993).

Third, in addition to these geochemical differences, the Nanga Parbat granites are in a different structural setting than the High Himalayan leucogranites. The granites occupy the core of a high-grade massif that has been recently uplifted and thrust over water-poor Kohistan basaltic rocks. Thus, the fluid-flux model of Le Fort and others (1987) cannot directly apply to the Nanga Parbat granites because they are not in a hot thrust over fertile unmetamorphosed schists.

Thus, the Nanga Parbat leucogranites are similar to the High Himalayan leucogranites in that they represent a near-minimum melt, probably produced by a mica breakdown reaction in a deep pelitic source rock (George, Harris, and Butler, 1993; Butler, Harris, and Whittington, 1997; Whittington, ms). However, the Nanga Parbat granites were formed much later than the High Himalayan leucogranites and their source was much more isotopically heterogeneous. We, thus, concur with earlier suggestions (Zeitler and Chamberlain, 1991; George, Harris, and Butler, 1993; Butler, Harris, and Whittington, 1997; Whittington, ms) that the leucogranite dikes and stocks in Nanga Parbat formed during decompression melting during the recent and rapid uplift of the massif.

EFFECTS OF FLUID-ROCK INTERACTION

Recent studies have shown that Nanga Parbat has experienced relatively intense hydrothermal activity during the past 10 my (Craw and others, 1994; Chamberlain and others, 1995; Butler, Harris, and Whittington, 1997). These studies suggest that a dual hydrothermal system exists at Nanga Parbat, dominated by meteoric waters in the upper portion of the crust and magmatic and/or metamorphic fluids in the lower, hotter crust. Fluid flow has clearly altered rocks within shear zones and has interacted to a far lesser degree with the gneisses, migmatite, and granites (Chamberlain and others, 1995).

Recently, a detailed study of micas in a shear zone along the edge of the massif showed that deformation and/or fluid flow have significantly affected the Rb-Sr systematics of both biotite and muscovite (George and Bartlett, 1996). We have extended the study of George and Bartlett (1996) into the highest-grade core of the massif to determine the effects of fluid flow there. Below, we propose that deposition of secondary calcite during hydrothermal activity and subsequent Sr exchange between carbonate minerals and biotite has significantly influenced the Rb/Sr systematics of granites and gneisses in the massif.

Our mineral Sr data can not be interpreted in terms of isochron ages because in 4 out of 6 samples of gneiss and migmatite, biotites have lower $^{87}Sr/^{86}Sr$ ratios than coexisting feldspars. Whole rock $^{87}Sr/^{86}Sr$ ratios are close to feldspar $^{87}Sr/^{86}Sr$ ratios because it is the largest Sr reservoir in the rock. Thus, feldspar–biotite–whole rock data yield negative ages on an isochron plot (fig. 5). Garnet Rb-Sr data (discussed below; fig. 6) further complicate the situation, having lower $^{87}Sr/^{86}Sr$ ratios than coexisting feldspar, but higher Rb/Sr ratios. Negative biotite-whole rock ages have been documented before in other areas of the NPHM by George, Reddy, and Harris (1995) and George and Bartlett (1996) who suggest that ductile deformation and/or fluid flow may be responsible for these disturbances. Elsewhere in the Himalayas, a negative biotite-whole rock Rb-Sr age was reported in gneiss from the Almora-Askot region of India (Powell and

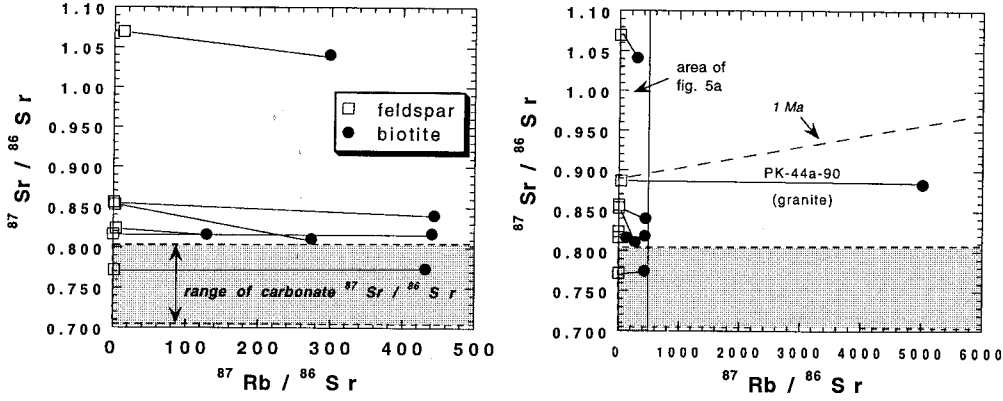

Fig. 5. $^{87}Rb/^{86}Sr$-$^{87}Sr/^{86}Sr$ isochron diagrams with feldspar (open squares) and biotite (black circles) mineral separate data for gneisses (A) and gneisses and granite (B) from Nanga Parbat. Solid lines connect coexisting minerals. Dashed line is 1 Ma reference isochron which includes present granite feldspar datum. Shaded area shows range of measured whole rock $^{87}Sr/^{86}Sr$ for carbonates/calcsilicates at Nanga Parbat.

others, 1979). Powell and others (1979) surmise that the biotite $^{87}Sr/^{86}Sr$ ratio was lowered by ^{87}Sr loss either during metamorphism or during incipient weathering.

Despite the negative isochron ages, we note that to the first order, biotite and feldspar in any given rock are relatively homogeneous in their $^{87}Sr/^{86}Sr$ ratios. That is, there are much smaller variations in $^{87}Sr/^{86}Sr$ between minerals than those between rocks (fig. 5), especially considering the wide range of Rb/Sr ratios in biotites. This relative homogeneity suggests either that Sr in previously-existing biotite has recently equilibrated with the larger feldspar Sr reservoir or that the biotite has recently formed in Sr isotopic equilibrium with the feldspar. In either case, this event represents a local equilibration of Sr in biotite and feldspar. This equilibration must have been quite recent, because the biotites have very high Rb/Sr ratios, and thus their $^{87}Sr/^{86}Sr$ ratios should increase rapidly once they are closed to Sr diffusion. For example, the $^{87}Sr/^{86}Sr$ ratio of biotite from sample PK-12a-90 should increase at a rate of 0.002 per my. Therefore, the near horizontal "isochrons" could only be maintained for timescales on the order of several million years. The large $^{87}Sr/^{86}Sr$ variation between samples indicates that this local equilibrium had a length scale greater than a hand sample ($\approx$20 cm) and smaller than the distance between samples (as small as 500 m).

Recent equilibration can explain biotite $^{87}Sr/^{86}Sr$ ratios equal to or slightly higher than feldspar ratios but can not explain biotite $^{87}Sr/^{86}Sr$ ratios that are lower than those of feldspar, as observed in 5 out of 7 of samples. Two possible explanations are that: (1) the feldspar $^{87}Sr/^{86}Sr$ ratio was somehow raised relative to that of coexisting biotite; or (2) biotite preferentially lost ^{87}Sr after the biotite-feldspar equilibration event. Because it is a decay product of Rb, ^{87}Sr in biotite is located in the loosely-bound interlayer sites more frequently than ^{86}Sr, which might account for preferential loss of ^{87}Sr. However, given the relative homogeneity of feldspar and biotite $^{87}Sr/^{86}Sr$ ratios within rocks, incongruent loss of ^{87}Sr seems less likely. If feldspar and biotite in these rocks have recently equilibrated, as indicated by this relative homogeneity, then it is likely that the Sr in both the interlayer and intralayer sites of biotite acquired the same $^{87}Sr/^{86}Sr$ ratio as the feldspar. Because this homogenization occurred within the last few million years and feldspar has a low Rb/Sr ratio, the present feldspar $^{87}Sr/^{86}Sr$ is still very close to the $^{87}Sr/^{86}Sr$ of homogenization. In this case, incongruent loss of Sr from interlayer sites in biotite would cause biotite $^{87}Sr/^{86}Sr$ ratios to approach the $^{87}Sr/^{86}Sr$ ratio of homogenization and thus would not cause the observed negative isochrons.

We believe that a third explanation is the most plausible: After the biotite-feldspar equilibration ended and feldspar became "closed" to Sr diffusion and exchange, the biotite $^{87}Sr/^{86}Sr$ ratio was lowered through exchange with a separate lower-$^{87}Sr/^{86}Sr$ reservoir. There are several possible reservoirs of low $^{87}Sr/^{86}Sr$: (1) apatite in the rocks themselves; (2) external fluids; and (3) carbonate minerals (including carbonate beds, minerals in calcsilicates, and secondary calcite veins) within the gneiss sequence. Apatite or external fluids are not large enough to be feasible reservoirs and can be ruled out by mass-balance considerations. Apatite is a trace mineral making up less than 1 percent of the rocks. Given a typical Sr concentration for apatite (1000 ppm), the total Sr reservoir in apatite is only slightly larger than the Sr reservoir in biotite, which makes up ≈30 percent of the gneisses and has a Sr concentration of 5 to 10 ppm. The feldspar-biotite equilibration event described above would be expected to equilibrate the Sr isotopes in apatite as well, because the Sr diffusion coefficient of apatite is higher than that of K-feldspar at temperatures of 650°C and lower (Giletti, 1991; extrapolated from measured diffusion parameters). Within 1 my after such an equilibration event, the $^{87}Sr/^{86}Sr$ ratio of biotite would increase much more rapidly than feldspar and apatite due to the much higher Rb/Sr ratio. At this point, a mass-balance calculation shows that equilibration between biotite and apatite would result in an $^{87}Sr/^{86}Sr$ ratio greater than that of feldspar.

Concentrations of Sr in waters–even high temperature waters such as the hot springs at Tato–are 10 to 100 times lower than Sr concentrations in biotite. Thus, if exchange with downward percolating meteoric waters, similar to the hot springs, has lowered the $^{87}Sr/^{86}Sr$ ratio of biotite in gneisses, and if the $^{87}Sr/^{86}Sr$ ratios of biotites and waters are equidistant from the final $^{87}Sr/^{86}Sr$ value, then 10 to 100 times more water than biotite would be needed. This volume of meteoric water is contrary to the observation that the oxygen isotopic signatures of most Nanga Parbat gneisses in the high-grade core of the massif do not show evidence for infiltration by large volumes of meteoric waters (Chamberlain and others, 1995).

Therefore, we suggest that carbonate minerals, either in secondary veins or in carbonate/calcsilicate beds, are the Sr reservoir that is most likely to have caused the low $^{87}Sr/^{86}Sr$ ratios in biotite. Our examination of over 150 thin sections of gneisses and granites in the core of the massif (Poage, unpublished data) show that disseminated calcite and calcite veinlets (<1 mm thick) are not uncommon throughout many of these rocks. The calcite is not a primary mineral in these rocks and is presumed to have been deposited by metamorphic and magmatic waters in the deeper portions of the hydrothermal system (Chamberlain and others, 1995). Approx 1 percent of the paragnesis sequence consists of carbonate and calcsilicate layers, which may be the source of the calcite veins. At present, we do not know if the exchange of Sr occurred at the outcrop level between carbonate lenses and gneisses or between disseminated secondary calcite within the rock. In either case the exchange must have been mediated by a relatively stagnant pore fluid, because calcite minerals are not in contact with biotites in all the samples analyzed. As opposed to an external surface-derived fluid that contains little Sr, the mediating fluid would effectively have a Sr concentration similar to that of the carbonates, because in this closed system it could carry Sr multiple times between the carbonate and biotite reservoirs. The fluid probably did not travel far (kilometers) because then one would expect to see more homogeneity in biotites between samples. We point out that there is abundant evidence for such a high-temperature metamorphic and/or magmatic fluid (Craw and others, 1994; Chamberlain and others, 1995; Winslow, Chamberlain, and Zeitler, 1995). Perhaps the most likely scenario is that a fluid whose chemical composition was buffered by the carbonate minerals in the carbonate and calcsilicate beds both exchanged Sr with biotites in the gneisses and granites and was responsible for the formation of secondary calcite veins.

Thus, we propose the following two-stage scenario to explain the observed mineral Sr isotope systematics. First, during the recent metamorphism the Sr in feldspar and in biotite exchanged and was isotopically homogenized. Second, following high-grade metamorphism the calcite veinlets were deposited by upward percolating magmatic/metamorphic fluids. After feldspar became closed to Sr exchange the $^{87}Sr/^{86}Sr$ ratio of biotite was lowered as a result of fluid-mediated interaction either with low $^{87}Sr/^{86}Sr$ carbonate/calcsilicate lenses or with secondary calcite veins in the granites and gneisses. Zuddas, Seimbille, and Michard (1995) determined experimentally that during granite-hydrothermal fluid interaction the contribution of biotite in determining the fluid $^{87}Sr/^{86}Sr$ ratio is most important during the initial stage of this interaction, whereas later the $^{87}Sr/^{86}Sr$ ratio of the fluid approaches that of the bulk rock as fluid-granite isotopic equilibrium is attained. This suggests that Sr in biotite is more easily exchanged with fluids than Sr in feldspar, consistent with our interpretation of the mineral isochrons and with experimentally determined diffusion parameters (Giletti, 1991). The fact that a 1 to 2 Ma leucogranite (zircon U-Pb age for PK-44a-90; Zeitler, Chamberlain, and Smith, 1993) displays similar biotite-feldspar Sr isotope systematics to the gneisses (fig. 5B) indicates that the Sr isotope exchange between biotite and carbonates has taken place in the last 2 my.

We point out that even the two samples whose biotite-feldspar data define positive slopes on a Rb-Sr isotopic evolution may have undergone exchange with carbonate. These two samples have the lowest whole rock $^{87}Sr/^{86}Sr$ ratios. One of these samples (PK-41a-90) was collected from the Tato shear zone, which experienced intense hydrothermal activity (Chamberlain and others, 1995). This sample displays strong evidence for hydrothermal alteration including abundant chlorite and iron-oxide alteration products. It is possible that feldspar in this particular sample did exchange Sr with the carbonates. Both these samples have whole rock $^{87}Sr/^{86}Sr$ ratios close to the range of carbonate $^{87}Sr/^{86}Sr$ ratios. Thus, another possibility is that the $^{87}Sr/^{86}Sr$ ratios of the carbonates were not low enough to pull the biotite values of these samples below the feldspar values.

If correct, our interpretation suggests that even though carbonates make up a small percentage (~1 percent) of the total rock in the massif, they have high enough Sr concentrations to buffer the Sr isotopic composition of biotite. Of the three carbonate/calcsilicate lenses we analyzed, two have sufficiently low $^{87}Sr/^{86}Sr$ ratios to bring biotite $^{87}Sr/^{86}Sr$ ratios below those of feldspar. The carbonate sample with the lowest $^{87}Sr/^{86}Sr$ ratio (JDB-TC) is from a massive block of marble, found as float on one of the moraines in the Tato drainage. The $^{87}Sr/^{86}Sr$ ratio of this sample (0.7058) appears to reflect a volcanic or marine source of Sr. The carbonate minerals in a calcsilicate rock (JDB-CS) have an $^{87}Sr/^{86}Sr$ ratio (0.8030) which might be expected after exchange of Sr with biotite in the calcsilicate. In addition, Blum and others (1998) measured the $^{87}Sr/^{86}Sr$ of secondary calcite in gneisses by leaching them in 4N acetic acid. They found that this calcite had $^{87}Sr/^{86}Sr$ values ranging from 0.7186 to 0.8236 indicating that: (1) the calcite veinlets have low enough $^{87}Sr/^{86}Sr$ values to cause a lowering of the $^{87}Sr/^{86}Sr$ of biotite during exchange, and (2) some of the calcite in the veinlets may have fully exchanged with the biotite.

Two other recent studies on Sr isotopes of carbonates elsewhere in the Himalayas (Harris and others, 1998; Singh and others, 1998) also found high leachate $^{87}Sr/^{86}Sr$ ratios and conclude that carbonates have probably attained these high $^{87}Sr/^{86}Sr$ ratios through exchange with silicates. However, for these studies and the study of Blum and others (1998), it is also possible that leaching, even with dilute acetic acid, causes incongruent dissolution of silicates, preferentially releasing ^{87}Sr from potassium sites. Harris and others (1998) addressed this question by leaching one sample with acids of different strength (10, 1, and 0.1 percent acetic acid). They saw little variation in the

$^{87}Sr/^{86}Sr$ ratio of the leachate, suggesting that leaching with the stronger acid did not release more ^{87}Sr than leaching with the weaker acids.

Hydrothermal activity and Sr exchange with carbonate, however, cannot alone explain the Rb-Sr data for the garnets examined in this study. Diffusion of Sr in garnet is extremely slow (Burton and others, 1995), and, thus, the $^{87}Sr/^{86}Sr$ ratio of garnet could not have been altered by post-metamorphic exchange with carbonate. Three of four garnets analyzed in this study have a lower $^{87}Sr/^{86}Sr$ than the weighted average of the feldspar and biotite and a higher Rb/Sr ratio than feldspar (fig. 6). We suggest three possible explanations for these garnet Rb-Sr systematics: (1) The garnets were formed during an earlier (Precambrian?) metamorphism. Because of the extremely slow diffusion of Sr in garnets, the garnet $^{87}Sr/^{86}Sr$ ratio was entirely unaffected by the recent homogenization of Sr (during recent metamorphism) that occurred between feldspar and biotite and the later exchange between biotite and carbonates. (2) The garnets may contain small apatite inclusions which have high concentrations of Sr and pre-date the metamorphism that resulted in garnet growth. (3) A portion of the garnets could have grown after the recent homogenization event and equilibrated with carbonate Sr in the same way as the biotite. We find apatite inclusions within some of the garnets, and there is evidence for at least two stages of garnet growth (Chamberlain, Jan, and Zeitler, 1989; Khattak, ms; Poage, unpublished data). Any combination of these three explanations is possible.

In the discussion above, we have described two recent Sr exchange events, a local equilibration between biotite and feldspar, followed by a lower temperature exchange between biotite and carbonate. Two simple calculations can be carried out to test the

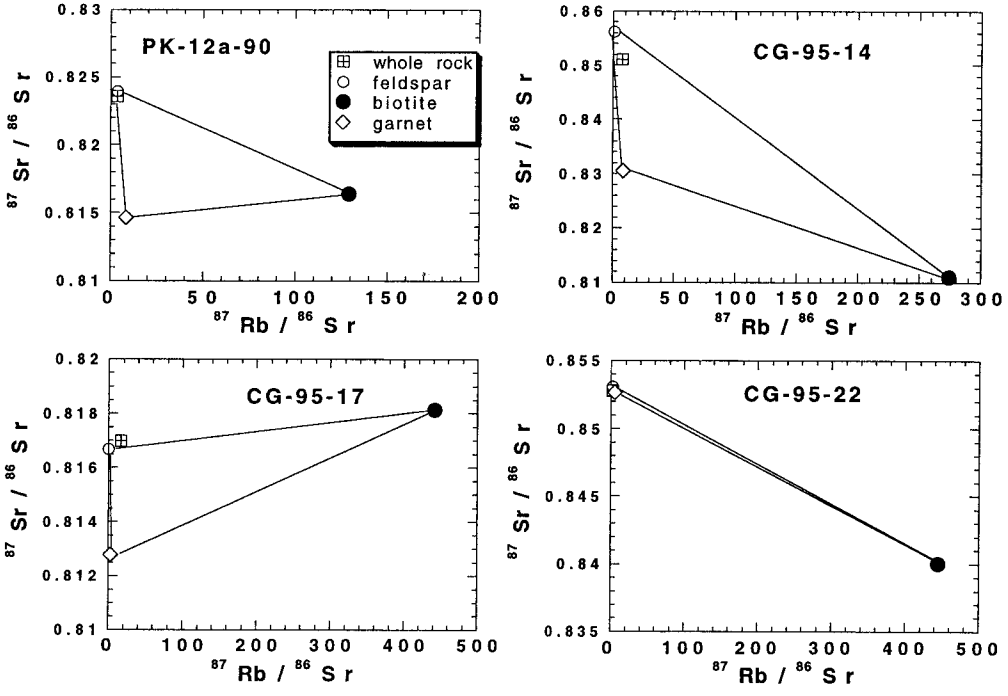

Fig. 6. $^{87}Rb/^{86}Sr$-$^{87}Sr/^{86}Sr$ isochron diagrams with mineral separate data for three gneiss samples (PK-12a-90, CG-95-14, and CG-95-17) and one migmatite leucosome sample (CG-95-22). Whole rock = crossed square; feldspar = open circle; biotite = black circle; garnet = open diamond; solid lines join coexisting mineral.

feasibility of our model. First, a mass balance calculation can be used to determine whether carbonate-biotite Sr exchange could produce the observed isotopic trends. We will assume that the modal abundances of biotite and calcite are 30 and 1% and that their Sr concentrations are 10 and 200 ppm, respectively. Although calcite is much less abundant than biotite, its contribution to the Sr mass balance is comparable because of its much higher Sr concentration. If 5 my passed after the feldspar-biotite equilibration event, then, assuming a typical biotite Rb/Sr ratio of 60, the biotite $^{87}Sr/^{86}Sr$ ratio would increase by approx 0.011 relative to the feldspar. In order to draw the biotite $^{87}Sr/^{86}Sr$ ratio back down below the feldspar ratio, a calcite $^{87}Sr/^{86}Sr$ ratio at least $\approx$0.02 lower than feldspar would be necessary. This is entirely feasible given the extremely radiogenic nature of the silicate Sr (feldspar $^{87}Sr/^{86}Sr \geq 0.7721$). Partial exchange with calcite having an $^{87}Sr/^{86}Sr$ ratio of 0.7500 or lower could easily produce the observed trends.

Secondly, we can use experimentally-determined Sr diffusion parameters for feldspars and biotites to test the hypothesis that Sr exchange between biotite and carbonate caused the negative Rb-Sr isochrons. In these calculations, we are interested in determining whether the Rb-Sr systematics of feldspar and biotite and their exchange with carbonate can be reproduced given a reasonable temperature/time history of the massif. In these calculations we seek to reproduce a situation where only 5 percent of the Sr in feldspar exchanges with carbonate whereas 90 percent of the Sr in biotite exchanges with carbonate. These percents were chosen to represent very little Sr exchange (essentially "closure") and nearly complete Sr exchange.

We will assume volume diffusion of Sr in both biotite and feldspar and that Sr transport in the pore fluid is extremely fast in comparison (Giletti, 1991; Zuddas, Seimbille, and Michard, 1995). Volume diffusion in biotite and feldspar is the slowest mechanism of exchange and thus an assumption that this was the dominant mechanism of exchange will tend to maximize the calculated timescale of exchange for a given temperature. Diffusion data for Sr in biotite and feldspar were taken from Hoffman and Giletti (1970) and Giletti (1991), respectively, and extrapolated to lower temperatures than those for which they were experimentally determined (625°-900°C) assuming an Arrhenius relationship. Sr exchange could have occurred between 300°C, the predicted closure temperature for biotite (for a cooling rate of 30°C/my; Jäger and Hunziker, 1979), and 700°C, the estimated melt temperature of the leucogranites (zircon and monazite thermometry; Butler, Harris, and Whittington, 1997). We will approximate the feldspar crystals as spheres and the biotite crystals as cylinders (transport parallel to layers), both with radii of 500 μm. Radii of feldspar and biotite crystals in NPHM rocks are similar, typically ranging from 100 to 800 μm. A 500 μm radius was chosen to be representative of larger crystals. Inasmuch as the diffusion length scale may actually be shorter than the grain radius, this choice will tend to maximize the calculated duration of exchange.

Solutions to the problem of diffusion in a sphere and in a cylinder are presented by Crank (1979). Figure 7 shows the time and temperature conditions for 5 percent exchange of Sr in feldspar and 90 percent exchange of Sr in biotite. To demonstrate the sensitivity to the percent-exchanged assumptions, curves are also shown for 25 percent exchange of Sr in feldspar and 60 percent exchange of Sr in biotite. Based on the above assumptions, it appears that exchange at temperatures below 350°C is too slow to account for even 60 percent exchange of Sr in biotite in the last several million years. At the other extreme, temperatures greater than 600°C could not be maintained for more that 10,000 yrs without exchange of greater than 25 percent of Sr in feldspar. It appears that our Rb-Sr data can be reproduced with the late cooling history of the Nanga Parbat massif, which is believed to have cooled from approx 700°C in the past 4 Ma (Smith, Chamberlain, and Zeitler, 1992; Whittington, 1996). However, we point out that uncertainties in the diffusion parameters can affect the calculated times by one or two

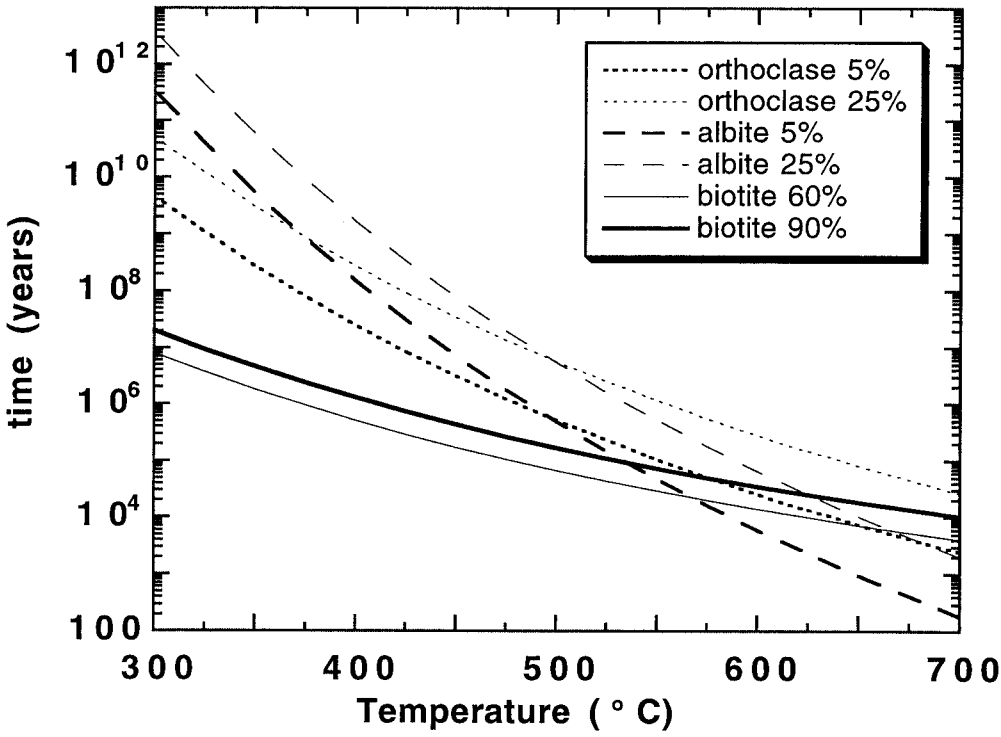

Fig. 7. Times and temperatures required to achieve 5 and 25 percent exchange of Sr in feldspar (dashed lines) and 90 and 60 percent exchange of Sr in biotite (solid lines). Assumptions are that exchange is through volume diffusion of Sr, that feldspar can be approximated by a sphere of radius 500 μm, and that biotite can be approximated by a cylinder of radius 500 μm. Diffusion parameters for Sr in feldspar and biotite are from Giletti (1991) and Hofmann and Giletti (1970). Solutions for diffusion in a sphere and cylinder are given in Crank (1956).

orders of magnitude, so this calculation does not serve to constrain the timescale of Sr exchange but rather to verify that the proposed scenario is consistent with experimentally derived diffusion parameters.

We believe that exchange of Sr between carbonate/calcsilicate lenses, secondary calcite, and biotite was fluid-mediated. The oxygen isotope data (Chamberlain and others, 1995; this study) serve to constrain the nature of the fluids involved in this Sr exchange. The fluid could not have been meteoric water, which has a much lower ^{18}O content than these rocks. Any interaction with meteoric water at high temperature would be expected to lower the $\delta^{18}O$ of feldspar, and this was not observed by Chamberlain and others (1995) except locally along faults and in several leucogranite samples. The hot springs at Nanga Parbat are meteoric in origin (Chamberlain and others, 1995), and they appear to carry Sr derived from silicates rather than carbonates based on their $^{87}Sr/^{86}Sr$ (table 2) and Ca/Sr ratios. These fluids may be responsible for local isotopic exchange along faults (Chamberlain and others, 1995), but they have not affected the bulk of the rock volume. The relatively high $^{87}Sr/^{86}Sr$ ratios of these hot springs are best explained by two factors: (1) the high temperature of the waters and their localization along fault zones where hydrothermal alteration is taking place; and (2) their relatively low Sr concentrations (1000 times lower than rocks) which makes them more susceptible to buffering by silicate Sr.

The heterogeneous nature of the Sr and oxygen isotopes in these rocks suggests that there was not a pervasive fluid flow system in them, because this would have homogenized the isotopic signatures. We believe that the local equilibration and exchange at Nanga Parbat were mediated by relatively stagnant pore fluids which were either metamorphic or magmatic in origin (see also Chamberlain and others, 1995; Winslow, Chamberlain, and Zeitler, 1995). These fluids would have $\delta^{18}O$ values in a range similar to the $\delta^{18}O$ values of rocks themselves (+9 to +12 ‰), and thus ^{18}O exchange at temperatures of 400° to 600°C with these fluids would not be expected to change substantially the bulk oxygen isotopic composition of the rocks.

CONCLUSIONS AND IMPLICATIONS

Three conclusions can be drawn from this data concerning the metamorphic/fluid flow history of the Nanga Parbat gneisses and the petrogenesis of the leucogranites.

First, whole rock $^{87}Sr/^{86}Sr$ and Rb/Sr ratios of gneisses confirm that they are derived from a Precambrian crustal source. The source rocks are isotopically heterogeneous, both in terms of Sr and oxygen isotopes, and are probably largely sedimentary in origin.

Second, the Nanga Parbat leucogranites have heterogeneous $^{87}Sr/^{86}Sr$ ratios within the range of the surrounding gneisses. However, the granites have lower $^{143}Nd/^{144}Nd$ ratios and $\delta^{18}O$ values than the surrounding gneisses. These isotopic signatures are best explained if the Nanga Parbat granites are derived from a similar but deeper crustal source rock. This conclusion is consistent with earlier suggestions that the leucogranite stocks and dikes were formed during vapor-absent melting (George, Harris, and Butler, 1993; Butler, Harris, and Whittington, 1997; Whittington, ms) possibly as a result of rapid decompression during uplift (Zeitler and Chamberlain, 1991).

Third, the Rb-Sr systematics of the gneisses and the granites have been strongly affected by Sr exchange with secondary, hydrothermal calcite and/or carbonate/calcsilicate lenses. We suggest that in the last few million years, during the recent young metamorphism, there was pervasive local homogenization of Sr isotopes between feldspar and biotite on a small (several meters?) scale. As the rocks cooled after high-grade metamorphism, feldspar, the largest Sr reservoir in these rocks, became effectively closed to Sr exchange. After this "closure," biotite continued to exchange Sr with either a magmatic or metamorphic fluid whose Sr isotopic composition was buffered by Sr in either sparsely interbedded calcsilicates and carbonates lenses or in secondary calcite veins. Stable isotopic (Chamberlain and others, 1995) and fluid inclusion (Winslow, Chamberlain, and Zeitler, 1995) studies suggest these fluids were metamorphic or magmatic in origin.

The observed exchange between carbonate and biotite has several important implications with regard to Rb-Sr systematics, in general, and Himalayan tectonics, in specific. Rubidium-Sr geochronology, particularly in high-grade metamorphic terranes, often yields ages that are inconsistent with other geochronologic techniques. Young Rb-Sr ages are often attributed to subsolidus fluid-rock interaction (Simonetti and Doig, 1990; Taylor and others, 1991; Kwan, Krähenbühl, and Jäger, 1992; Juteau and others, 1984). In this study, we have examined the Rb-Sr isotope systematics in a region that has undergone metamorphism and melting recently. We propose a mechanism by which these Rb-Sr systematics may become distorted. Slopes of biotite-feldspar pairs on a Rb-Sr isotopic evolution diagram (fig. 5) define apparent ages ranging from +0.4 to −11.7 Ma. If these minerals remain closed to diffusion of Rb and Sr, then 90 my in the geologic future, they will yield ages that range from 78 to 90 Ma. If these rocks are in fact 10 my old at present, the Rb-Sr mineral isochrons will yield ages 10 to 22 percent lower than the true age (100 Ma). Thus, the mechanism we propose can be responsible for large discrepancies between the apparent Rb-Sr age and the true age of a rock, and this should

be considered in Rb-Sr geochronologic studies, especially when there are carbonates in the study area.

The exchange of Sr between biotite and carbonates could also have significant implications for the interpretation of the seawater Sr curve, because it enables carbonates to contribute radiogenic Sr to the dissolved load in streams. A dramatic rise in the $^{87}Sr/^{86}Sr$ ratio of marine carbonates in the past 40 my has been attributed to weathering in the Himalayan mountain belt, which contributes increased amounts of radiogenic strontium to the ocean (Edmond, 1992). Measured $^{87}Sr/^{86}Sr$ ratios of Himalayan streams within the Ganges-Brahmaputra and Indus River drainage systems are significantly higher than waters from large streams elsewhere (Palmer and Edmond, 1989; Krishnaswami and others, 1992; Harris and others, 1998).

The lithologic source of the radiogenic strontium in Himalayan streams has been debated. A silicate source could have a significant effect on the climate because weathering of silicate minerals consumes atmospheric CO_2 (Raymo, Ruddiman, and Froelich, 1988; Raymo and Ruddiman, 1992). Based on a study of the Rb-Sr systematics of waters in the Ganges-Brahmaputra river system, Krishnaswami and others (1992) argue that the $^{87}Sr/^{86}Sr$ ratios of these waters are predominantly the result of intense weathering of Precambrian granites and gneisses; that is, dominantly silicate weathering. Edmond (1992) suggested that metamorphism had remobilized Sr from K-rich minerals to Ca- and Na-rich minerals and that weathering of these minerals from unroofed metamorphic core complexes was contributing to the rise in marine $^{87}Sr/^{86}Sr$. Palmer and Edmond (1992), suggested that metamorphism had repartitioned elements such that Himalayan carbonates are unusually radiogenic ($^{87}Sr/^{86}Sr > 0.7200$).

In this study and in Blum and others (1998) we have found evidence to support the hypothesis of Palmer and Edmond (1992). In the Nanga Parbat-Haramosh Massif, it appears that radiogenic strontium has been transferred from silicate minerals (mainly biotite) to calcite. The carbonates, although representative of only a small proportion of the rocks, weather more readily than the surrounding gneiss and contribute the majority of the Sr flux in streams. Major element and Sr isotope data for spring and river waters from the Raikot drainage support this proposed scenario (Blum and others, 1998). Future work is necessary to determine whether this silicate-carbonate exchange is occurring on a larger (Himalayan) scale.

ACKNOWLEDGMENTS

The authors wish to thank Peter Zeitler for his continued collaboration and encouragement during the course of this project. Patrick LeFort and two anonymous reviewers provided constructive comments which have greatly improved this manuscript. We also thank Syed Hamidullah, Jeff Hashimoto, Asif Khan, Arnaud Pechet, and Mike Hingston for sharing in discussions, field work, and sample collection. Financial support for this study was provided by NSF grant EAR-9418154 (to Chamberlain and Blum) and is part of the Nanga Parbat Continental Dynamics Project.

REFERENCES

Blattner, P., Dietrich, V., and Gansser, A., 1983, Contrasting ^{18}O enrichment and origins of High Himalayan and Trans-himalayan intrusives: Earth and Planetary Science Letters, v. 65, p. 276–286.

Blum, J. D., Gazis, C. A., Jacobsen, A. D., and Chamberlain, C. P., 1998, Carbonate versus silicate weathering in the Raikot watershed within the High Himalayan crystalline series: Geology, v. 26, p. 411–414.

Burton, K. W., Kohn, M. J., Cohen, A. S., and O'Nions, R. K., 1995, The relative diffusion of Pb, Nd, Sr and O in garnet: Earth and Planetary Science Letters, v. 133, p. 199–211.

Butler, R. W. H., George, M., Harris, N. B. W., Jones, C., Prior, D. J., Treolar, P. J., and Wheeler J., 1992, Geology of the northern part of the Nanga Parbat massif, northern Pakistan, and its implications for Himalayan tectonics: Journal of the Geological Society of London, v. 149, p. 557–567.

Butler, R. W. H., Harris, N. B. W., and Whittington, A. G., 1997, Interactions between deformation, magmatism and hydrothermal activity during active crustal thickening: a field example from Nanga Parbat, Pakistan Himalayas: Mineralogical Magazine, v. 61, p. 37–52.

Butler, R. W. H., and Prior, D. J., 1988, Tectonic controls on the uplift of the Nanga Parbat Massif, Pakistan Himalayas: Nature, v. 333, p. 247–250.

Chamberlain, C. P., Jan, M. Q., and Zeitler, P. K., 1989, A petrologic record of the collision between the Kohistan Island-Arc and Indian Plate, northwest Himalaya, in Malinconico, L. L., and Lillie, R. J., editors, Tectonics of the Western Himalayas: Geological Society of America Special Paper 232, p. 23-32.

Chamberlain, C. P., Zeitler, P. Z., Barnet, D. E., Winslow, D., Poulson, S. R., Leahy, T., and Hammer, J. E., 1995, Active hydrothermal systems during the recent uplift of Nanga Parbat, Pakistan Himalaya: Journal of Geophysical Research, v. 100, p. 439–453.

Chamberlain, C. P., Zeitler, P. K., and Erickson, E., 1991, Metamorphism at Babusar Pass, northern Pakistan: implications for the metamorphic evolution of the northwestern Himalaya: Journal of Petrology, v. 99, p. 829–849.

Coward, M. P., Butler, R. W. H., Chambers, A. F., Graham, R. H., Izatt, C. N., Khan, M. A., Knipe, R. J., Prior, D. J., Treloar, P. J., and Williams, M. P., 1988, Folding and imbrication if the Indian crust during Himalayan collision: Philosophical Transactions of the Royal Society of London, v. A326, p. 89–116.

Coward, M. P., Butler, R. W. H., Khan, M. A., and Knip,e R. J., 1987, The tectonic history of Kohistan and its implications for Himalayan structure: Journal of the Geological Society of London, v. 188, p. 385–433.

Coward, M. P., Jan, M., Rex, D., Tarney, J., Thirwall, M., and Windley, B. F., 1982, The tectonic history of Kohistan and its implications for Himalayan structure: Journal of the Geological Society of London, v. 139, p. 299–308.

Coward, M. P., Windley, B. F., Broughton, R. D., Luff, I. W., Petterson, M. G., Pudsey, C. J., Rex, D. C., and Khan, M. A., 1986, Collision tectonics in the NW Himalayas, in Coward, M. P., and Ries, A. C., editors, Collision Tectonics: Geological Society of London Special Publication 19, p. 203–219.

Crank, J., 1956, The Mathematics of Diffusion: London, Oxford University Press, 347 p.

Craw, D., Koons, P. O., Winslow, D., Chamberlain, C. P., and Zeitler, P. K., 1994, Boiling fluids in a region of rapid uplift, Nanga Parbat Massif, Pakistan: Earth and Planetary Science Letters, v. 128, p. 169–182.

Criss, R. E., Gregory, R. T., and Taylor, H. P., Jr., 1987, Kinetic theory of oxygen isotopic exchange between minerals and water: Geochímica et Cosmochimica Acta, v. 51, p. 1099–1108.

Debon, F., Le Fort, P., Sheppard, S. M. F., and Sonet, J., 1986, The four plutonic belts of the Transhimalaya-Himalaya: a chemical-mineralogical, isotopic and chronological synthesis along a Tibet-Nepal section: Journal of Petrology, v. 27, p. 219–250.

Deniel, C., Vidal, P., Fernandez, A., Le Fort, P., and Peucat, J. J., 1987, Isotopic study of the Manaslu granite (Himalaya, Nepal): inferences on the age and source of Himalayan leucogranites: Contributions to Mineralogy and Petrology, v. 96, p. 78–92.

Dietrich, V., and Gansser, A., 1981, The leucogranites of the Bhutan Himalaya (crustal anatexis versus mantel melting): Bulletin Suisse de Minéralogie et Petrographie, v. 61, p. 177–202.

Edmond, J. M., 1992, Himalayan tectonics, weathering processes, and the strontium isotope record in marine limestones: Science, v. 258, p. 1594–1597.

Ferrara, G., Lombardo, B., and Tonarini, S., 1983, Rb/Sr geochronology of granites and gneisses from the Mount Everest region, Nepal Himalaya: Geologische Rundschau, v. 72, p. 119–136.

Gansser, A., 1983, Geology of the Bhutan Himalaya: Mémoires de la Société Helvétiques des Sciences Naturelles, v. 96, p. 181.

George, M. T., ms, 1993, The magmatic, thermal and exhumation history of the Nanga Parbat Haramosh Massif, Western Himalaya: Ph.D. thesis, Open University, 402 p.

George, M. T., and Bartlett, J. M., 1996, Rejuvenation of Rb-Sr mica ages during shearing on the northwestern margin of the Nanga Parbat-Haramosh massif: Tectonophysics, v. 260, p. 167–185.

George, M. T., Harris, N. B. W., and Butler, R. W. H., 1993, The tectonic implications of contrasting granite magmatism between the Kohistan island arc and the Nanga Parbat-Haramosh Massif, Pakistan Himalaya, in Searle, M. P. and Treolar, P. J., editors, Himalayan Tectonics: Geological Society of London Special Publication 74, p. 173–191.

George, M. T., Reddy, S., and Harris, N. B. W., 1995, Isotopic constraints on the cooling history of the Nanga Parbat-Haramosh Massif and Kohistan Arc, western Himalaya: Tectonics, v. 14, p. 237–252.

Giletti, B. J., 1991, Rb and Sr diffusion in alkali feldspars, with implications for cooling histories: Geochimica et Cosmochimica Acta, v. 55, p. 1331–1343.

Harris, N., Ayres, M., and Massey, J., 1995, Geochemistry of granitic melts produced during the incongruent melting of muscovite: Implications for the extraction of Himalayan leucogranite magmas: Journal of Geophysical Research, v. 100, p. 15767–15777.

Harris, N., Bickle, M., Chapman, H., Fairchild, I., and Bunbury, J., 1998, The significance of Himalayan rivers for silicate weathering rates: evidence from the Bhote Kosi tributary: Chemical Geology, v. 144, p. 205–220.

Harris, N., Inger, S., and Massey, J., 1993, The role of fluids in the formation of High Himalayan leucogranites, in Searle, M. P. and Treolar, P. J., editors, Himalayan Tectonics: Geological Society of London Special Publication 74, p. 391–400.

Hess, P. C., 1989, Origins of Igneous Rocks: Cambridge, Harvard University Press, 336 p.

Hofmann, A. W., and Giletti, B. J., 1970, Diffusion of geochronologically important nuclides under hydrothermal conditions: Eclogae Geologicae Helvetiae, v. 63, p. 141–150.

Inger, S., and Harris, N., 1993, Geochemical constraints on leucogranite magmatism in the Langtang Valley, Nepal Himalaya: Journal of Petrology, v. 34, p. 345–368.

Jäger, E., and Hunziker, J. C., 1979, Lectures in Isotope Geology: New York, Springer-Verlag, 329 p.

Juteau, M., Michard, A., Zimmermann, J.-L., and Albarede, F., 1984, Isotopic heterogeneities in the granitic intrusion of Monte Capanne (Elba Island, Italy) and dating concepts: Journal of Petrology, v. 25, p. 532–545.

Khattak, W. U. K., ms, 1995, Petrology and stable isotope geochemistry of the Nanga-Parbat-Haramosh Massif, Northern Pakistan: Ph.D. thesis, University of South Carolina, 158 p.

Krishnaswami, S., Trivedi, J. R., Sarin, M. M., Ramesh, R., and Sharma, K. K., 1992, Strontium isotopes and rubidium in the Ganga-Brahmaputra river system: Weathering in the Himalaya, fluxes to the Bay of Bengal and contributions to the evolution of oceanic $^{87}Sr/^{86}Sr$: Earth and Planetary Science Letters, v. 109, p. 243–253.

Kwan, T. S., Krähenbühl, R., and Jäger, E., 1992, Rb-Sr, K-Ar and fission track ages for granites from Penang Island, West Malaysia: an interpretation model for Rb-Sr whole-rock and for actual and experimental mica data: Contributions to Mineralogy and Petrology, v. 111, p. 527–542.

Le Fort, P., Cuney, C., Deniel, C., France-Lanord, C., Sheppard, S. M. F., Upreti, B. N., and Vidal, P., 1987, Crustal generation of the Himalayan leucogranites: Tectonophysics, v. 134, p. 39–57.

Madin, I. P., Lawrence, R. D., and Ur-Rehman, S., 1989, The northwestern Nanga Parbat-Haramosh Massif: Evidence for crustal uplift at the northwestern corner of the Indian craton. in Malinconico, L. L., and Lillie, R. J., editors, Tectonics of the Western Himalayas: Geological Society of America Special Paper 232, p. 169–182.

Maluski, H., and Matte, P., 1984, Ages of Alpine tectonometamorphic events in the northwestern Himalaya (northern Pakistan) by $^{40}Ar/^{39}Ar$ method: Tectonics, v. 3, p. 1–18.

Massey, J. A., Harmon, R. S., and Harris, N. B. W., 1994, Contrasting retrograde oxygen isotope exchange behaviour and implications: examples from the Langtang Valley, Nepal: Journal of Metamorphic Geology, v. 12, p. 261–272.

Misch, Peter, 1949, Metasomatic granitization of batholithic dimensions: American Journal of Science, v. 247, p. 209–249.

Palmer, M. R., and Edmond, J. M., 1989, The strontium isotope budget of the modern ocean: Earth and Planetary Science Letters, v. 92, p. 11–26.

Pognante, U., Benna, P., and Le Fort, P., 1993, High-pressure metamorphism in the High-Himalayan Crystallines of the Stak Valley, northeastern Nanga Parbat-Haramosh Syntaxis, Pakistan, in Searle, M. P. and Treolar, P. J., editors, Himalayan Tectonics: Geological Society of London Special Publication 74, p. 161–172.

Powell, C. M., Crawford, A. R., Armstrong, R. L., Prakash, R., and Wynne-Edwards, H. R., 1979, Reconnaissance Rb-Sr dates for the Himalayan Central Gneiss, northwest India: Indian Journal of Earth Science, v. 6, p. 139–151.

Raymo, M. E., and Ruddiman, W. F., 1992, Tectonic forcing of the late Cenozoic climate: Nature, v. 359, p. 117–122.

Raymo, M. E., Ruddiman, W. F., and Froelich, P. N., 1988, Influence of late Cenozoic mountain building on ocean geochemical cycles: Geology, v. 16, p. 649–653.

Scaillet, B., France-Lanord, C., and Le Fort, P., 1990, Badrinath-Gangotri plutons (Garhwal, India): petrological and geochemical evidence for fractionation processes in a high Himalayan leucogranite: Journal of Volcanology and Geothermal Research, v. 44, p. 163–188.

Searle, M. P., and Fryer, B. J., 1986, Garnet, tourmaline and muscovite-bearing leucogranites of the Higher Himalaya from Zanskar, Kulu, Lahoul and Kashmir, in Coward, M. P., and Ries, A. C., editors, Collision Tectonics: Geological Society of London Special Publication 19, p. 185–201.

Sheppard, S. M. F., 1986, Igneous Rocks: III. Isotopic case studies of magmatism in Africa, Eurasia, and oceanic islands, in Valley, J. W., Taylor, H. P., Jr., and O'Neil, J. R., editors, Stable Isotopes in High Temperature Geological Processes: Reviews in Mineralogy 16, p. 319–372.

Sheppard, S. M. F., Debon, F., Liu, G. H., Jin, C. W., and Xu, R. H., 1983, Oxygen isotope relationships in three plutonic belts in Southern Tibet: Terra Cognita, v. 3, p. 272.

Simonetti, A., and Doig, R., 1990, U-Pb and Rb-Sr geochronology of Acadian plutonism in the Dunnage zone of the southeastern Quebec Appalachians: Canadian Journal of Earth Science, v. 27, p. 881–892.

Singh, S. K., Trivedi, J. R., Pande, K., Ramesh, R., and Krishnaswami, S., 1998, Chemical and strontium, oxygen, and carbon isotopic compositions of carbonates from the Lesser Himalaya: Implications to the strontium isotope composition of the source waters of the Ganga, Ghaghara, and Indus rivers: Geochimica et Cosmochimica Acta, v. 62, p. 743–755.

Smith, H. A., Chamberlain, C. P., and Zeitler, P. K., 1992, Documentation of Neogene regional metamorphism in the Himalayas of Pakistan using U-Pb in monazite: Earth and Planetary Science Letters, v. 113, p. 93–105.

Tahirkheli, F. A. K., Mattauer, M., Proust, F., and Tapponnier, P., 1979, The India-Eurasia suture zone in northern Pakistan: some new data for an interpretation at plate scale, *in* Farah and Dejong, K. A. editors, Geodynamics of Pakistan: Quetta, Geological Survey of Pakistan, p. 130–135.

Taylor, P. N., Kramers, J. D., Moorbath, S., Wilson, J. F., Orpen, J. L., and Martin, A., 1991, Pb/Pb, Sm-Nd and Rb-Sr geochronology in the Archean Craton of Zimbabwe: Chemical Geology, v. 87, p. 175–196.

Taylor, R. T., and McLennan, S. M., 1985, The continental crust: its composition and evolution: Oxford, Blackwell Scientific, 312 p.

Treloar, P. J., and Izatt, C. N., 1993, Tectonics of the Himalayan collision between the Indian Plate and the Afghan block: a synthesis, in Searle, M. P., and Treolar, P. J., editors, Himalayan Tectonics: Geological Society of London Special Publication 74, p. 69–87.

Treloar, P. J., Rex, D. C., Guise, P. G., Coward, M. P., Searle, M. P., Windley, B. F., Petterson, M. G., Jan, M. Q., and Luff, I. W., 1989, K-Ar and Ar-Ar geochronology of the Himalayan collision in NW Pakistan: constraints on the timing of suturing, deformation, metamorphism, and uplift: Tectonics, v. 8, p. 881–909.

Treloar, P. J., Wheeler, J., and Potts, G. J., 1994, Metamorphism and melting within the Nanga Parbat syntaxis, Pakistan Himalaya: Mineralogical Magazine, v. 58A, p. 910–911.

Vidal, P., Bernard-Griffiths, J., Cocherie, A., and Le Fort, P., 1984, Geochemical comparison between Himalayan and Hercynian leucogranites: Physics of Earth and Planetary Interiors, v. 35, p. 179–190.

Wang, J. W., Chen, Z. L., Gui, X. T., Xu, R. H., and Zhang, Y. Q., 1981, Rb-Sr isotopic studies on some intermediate-acid plutons in Southern Xizang, in Geological and Ecological studies of Qinghai-Xizang Plateau-Symposium Beijing: Beijing, Science Press, p. 515–520.
Wheeler, J., Treolar, P. J., and Potts, G. J., 1995, Structural and metamorphic evolution of the Nanga Parbat syntaxis, Pakistan Himalayas, on the Indus gorge transect: the importance of early events: Geological Journal, v. 30, p. 349–371.
Whittington, A. G., 1996, Exhumation overrated at Nanga Parbat: Tectonophysics, v. 206, p. 215–226.
——— ms, 1997, The thermal, metamorphic and magmatic evolution of a rapidly exhuming terrane: the Nanga Parbat Massif, northern Pakistan: Ph.D thesis, The Open University, 432 p.
Winslow, D. M., Chamberlain, C. P., and Zeitler, P. K., 1995, Metamorphism and melting of the lithosphere due to rapid denudation, Nanga Parbat Massif Himalaya: Journal of Geology, v. 103, p. 395–409.
Winslow, D. M., Zeitler, P. K., Chamberlain, C. P., and Hollister, L. S., 1994, Direct evidence for a steep geotherm under conditions of rapid denudation, Western Himalaya, Pakistan: Geology, v. 22, p. 1075–1078.
Zeitler, P. K., 1985, Cooling history of the NW Himalaya, Pakistan: Tectonics, v. 4, p. 127–151.
Zeitler, P. K., and Chamberlain, C. P., 1991, Petrogenetic and tectonic significance of young leucogranites from the northwestern Himalaya, Pakistan: Tectonics, v. 10, p. 729–741.
Zeitler, P. K., Chamberlain, C. P., and Smith, H. A., 1993, Synchronous anatexis, metamorphism, and rapid denudation at Nanga Parbat (Pakistan Himalaya): Geology, v. 21, p. 347–350.
Zeitler, P. K., Sutter, J. F., Williams, I. S., Zartman, R., and Tahirkheli, R. A. K., 1989, Geochronology and temperature history of the Nanga-Parbat-Haramosh massif, Pakistan: in Malinconico, L. L., and Lillie, R. J., editors, Tectonics of the Western Himalayas: Geological Society of America Special Paper 232, p. 1–22.
Zuddas, P., Seimbille, F., and Michard, G., 1995, Granite-fluid interaction at near-equilibrium conditions: Experimental and theoretical constraints from Sr contents and isotopic ratios: Chemical Geology, v. 121, p. 145–154.